ABSTRACT

PARTIAL CHARACTERIZATION OF EXTRUDED COLLAGEN TUBES WITH VARIED MATERIAL DEPOSITION AND ORIENTATION BASED ON ROTATION RATE AND LINEAR DRAW SPEED

by
Richard Peter Hoppe

This study established protocols for extrusion of collagen tubes from an extruder made by the ZOKO Corporation of Czechoslovakia. Using a viscous collagen base material, collagen tubes can be formed with changes in rotation rates from 0 rpm to 260 rpm and linear draw speeds from 383 mm/min to 1270 mm/min with a constant extrusion rate of 50 cm^2/min. These tubes, with further research and treatment, can be used for various medical applications including vascular implants and nerve conduits.

Post-extrusion, chemical crosslinking of the collagen increased the cohesiveness and mechanical integrity of the tubes. Microscopic photographs confirmed higher orientation of the fibers on the surface with less orientation on the interior surface of the tube. The collagen tubing displayed high affinity for water and was able to change mass by at least 100%. The tube volume changes ranged from 80% to 123% with length changes from 8% to 13% depending on thickness of the tube and the applied rotation rate.

The tensile properties supported the idea of collagen as a short fiber-reinforced material. The maximum tensile strength was attained with low to medium rotation rate and a medium thickness tube. There was increased modulus of the initial toe region and a decreased end region modulus as the rotation rate increased.

Thermal analysis showed differences between the shapes of energy versus temperature curves when comparing the tubes which were "normal" and those which were dehydrated before testing. Distinct water peaks increased in range for non-dehydrated and decreased for dehydrated tubes with increasing rotation rate. An exothermic region also appeared which was either some form of shrinkage or denaturing/degradation of the collagen molecules. The actual degradation of the material had a beginning range of temperatures from 250° C to 257° C which apparently increased with increasing rotation rate.

PARTIAL CHARACTERIZATION OF EXTRUDED COLLAGEN TUBES WITH VARIED MATERIAL DEPOSITION AND ORIENTATION BASED ON ROTATION RATE AND LINEAR DRAW SPEED

by
Richard Peter Hoppe

A Thesis
Submitted to the Faculty of
New Jersey Institute of Technology
In Partial Fulfillment of the Requirements for the Degree of
Master of Science in Biomedical Engineering

Department of Biomedical Engineering

May 2001

APPROVAL PAGE

PARTIAL CHARACTERIZATION OF EXTRUDED COLLAGEN TUBES WITH VARIED MATERIAL DEPOSITION AND ORIENTATION BASED ON ROTATION RATE AND LINEAR DRAW SPEED

Richard Peter Hoppe

May 9, 2001

Dr. Michael Jaffe, Thesis Advisor — Date
Professor of Biomedical Engineering, NJIT

Dr. David Kristol, Committee Member — Date
Professor of Biomedical Engineering, NJIT

Dr. Louis Barash, Committee Member — Date
Adjunct Professor of Chemistry, NJIT

BIOGRAPHICAL SKETCH

Author: Richard Peter Hoppe

Degree: Master of Science in Biomedical Engineering

Date: May 2001

Undergraduate and Graduate Education:

- Master of Science in Biomedical Engineering,
  New Jersey Institute of Technology, Newark, NJ, 2001

- Bachelor of Science in Engineering Science
  New Jersey Institute of Technology, Newark, NJ, 1999

Major: Biomedical Engineering

To my beloved family who supported me throughout this grand endeavor.
In loving memory of my father Kurt William Hoppe Sr.
(December 5, 1942 – August 8, 2000)

ACKNOWLEDGMENTS

I would like to express my deepest appreciation to Dr. Michael Jaffe, who served as my thesis advisor and research supervisor and provided me with valuable assistance in the completion of this paper. I would also like to give special thanks to Dr. David Kristol and Dr. Lou Barash for serving as members of my committee.

I would also like to thank Dr. Sal Romano, Dr. Victor Tan, Dr. Robert Marder, Nels Lauritzen, Peter Espino, Joseph Pickton and Ronald Kafchinski for their assistance in the research and testing done for this thesis.

I would like to thank my boss, Arely Sequeira, for allowing me time to work on this thesis and giving words of encouragement when things dragged.

I would also like to thank Ivory Kilpatrick for helping me finally finish this paper and keeping me on track as well as for serving as an unofficial committee member and an ear to listen to my complaints and joys.

Finally, I would like to thank Sharon Toscano for keeping me motivated and on track and supporting me every step of the way. Thanks to Judith Kapp for always having kind words and good stories to help me get my mind off of the research. Gratitude and good luck to Rehan Khanzada and Joseph Valdellon for working with me in the lab and making these collagen tubes work. Last but not least, my family, for their assistance and constant belief in my abilities and their support over the years.

TABLE OF CONTENTS

TABLE OF CONTENTS
(Continued)

LIST OF TABLES

LIST OF TABLES
(Continued)

LIST OF FIGURES

CHAPTER 1

INTRODUCTION

A major component of body make-up material are proteins arranged in various polypeptide forms. The most prevalent is collagen which is the primary fibrinous component of connective tissue. Collagen is found throughout the body in many different forms. It helps provide structure and support to skin, blood vessels, and muscles. Since it has so many forms and uses, collagen becomes a good choice for biomedical applications provided it can be shaped to mimic various body parts. A second important factor is its ability to maintain adequate properties, be it mechanical or chemical, in order to allow it to perform in the intended application. One of the possible uses is in replacement of blood vessels or other hollow body organs such as the larynx or ureters by way of collagen shaped into tubes.

1.1 Collagen Overview

Collagen itself is a complex protein that can be found in many forms within the body and is a major constituent in skin, bone, tendon, and other connective tissues. To date, at least ten varieties of collagen have been identified with various functions and properties (1). What makes these different forms all collagen is the distinctive molecular structure of a triple helix with an abundance of the residue glycine arranged in a triplet of Gly–X–Y. For collagen, the X and Y are mainly proline and hydroxyproline which help direct the chain configuration through their rigidity (1). The presence of glycine is essential as every third residue for steric reasons. Glycine's small side chain allows for the formation of the triple helix. The other amino acids which make up the protein are dependent upon the species in which it is found. A listing of the amino acids of collagens from different

species can be seen in table 1.1 (2). The general shape of the collagen, whether it is fibrillar or non-fibrillar as well as the length of the helix and the size of the non-helical portions, helps to determine what function it performs in the body (3). The collagen molecule is rod shaped and is approximately 3000 Å long and 14 Å in diameter which is composed of three polypeptide chains in a triple helix form. The terminal peptide regions, known as the telopeptide segments, do not form a triple helix and is the main site for crosslinking. Figure 1.1 shows the molecular structure of type I procollagen. A general chemical structure can be seen in figure 1.2.

Table 1.1 Amino acids of various species (per 1000 residues).

Amino Acid	Calf Skin	Rat Skin	Human Tendon	Shark Skin
Alanine	112	106	110.7	119
Glycine	320	327	324	333
Valine	20	22	25.4	21.9
Leucine	25	25	26	23.9
Isoleucine	11	10	11.1	19.4
Proline	138	117	126.4	113.4
Phenylalanine	13	13	14.2	13.9
Tyrosine	2.6	3.2	3.6	1.4
Serine	36	41	36.9	44.5
Threonine	18	20	18.5	25.8
Methionine	4.3	6.3	5.7	10
Arginine	50	49	49.0	50.3
Histidine	5.0	5.1	5.4	7.4
Lysine	27	29	21.6	24.3
Aspartic Acid	45	47	48.4	42.6
Glutamic Acid	72	74	72.3	65.8
Hydroxyproline	94	100	92.1	78.5
Hydroxylysine	7.4	5.7	8.9	4.7
Cystine				
Amide Groups	46	51	44	29.4

Source: Mark, H., Gaylord, N., and Bikales, N., Collagen in Encyclopedia of Polymer Science and Technology, Interscience Publishers, N.Y., 1-15, 1966.

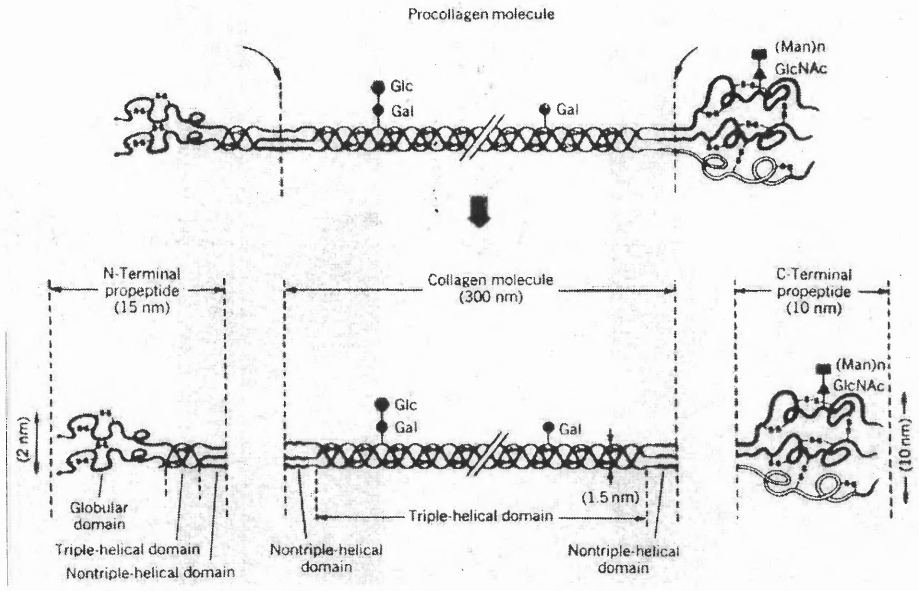

Figure 1.1 General chemical structure of a procollagen molecule showing the main helical portion with a propeptide region on either end and a triple helical region in the center. The collagen molecules align to form the fibrils and then further align to form fibers and fiber networks. Source: Kroschwitz, J., Collagen in Encyclopedia of Polymer Science and Engineering, Volume 3, Wiley Interscience Publishers, N.Y., 699-725, 1985.

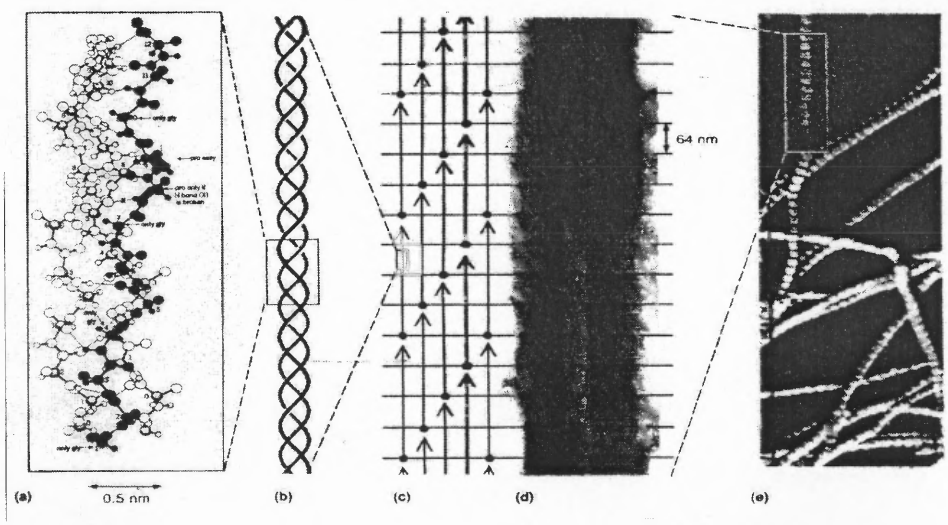

Figure 1.2 Chemical structure of collagen and assembly into molecules and finally fibers. (a) Represents the amino acid level to show the arrangement making up the tropocollagen fibril seen in (b). The fibrils then align in a head to tail overlapping section seen in (c). The picture in (d) originally showed the full length fiber which then arranges into a fibrous network seen in (e).
Source: Mathews, C., van Holde, K.E., The three-dimensional structure of proteins in Biochemistry, Benjamin Cummings Publishing Co., MA., 183-184, 1990.

Another commonality of collagens which can be observed in their bulk form is the tendency to swell when immersed in an acid. In addition, collagens are usually inelastic and have a higher resistance to degradation by proteolytic enzymes, which act on the telopeptide region, but are susceptible to the enzyme collagenase. The collagenases are able to break up the main helical region of collagen. This is accomplished by a series of enzymes that operate under physiological conditions (pH and temperature) that can create the critical cleavage in the helical body of the molecule within the fibril (4). The mammalian collagenase cleaves at a specific location between glycine 775 and isoleucine 776 (5). These leave two portions which are ¼ and ¾ the original length. The molecule is then susceptible to attack by other enzymes which completely break the protein into its component amino acids. According to Ramachandran, "there is no evidence for separate collagenases for the different collagen types" (4). Cross-linking, however, which will be discussed later, is able to slow the collagenase action by preventing the complete breakdown of the molecule after the initial cleavage. Finally, collagens, which are normally insoluble, can be converted into a soluble gelatin by prolonged exposure to temperatures above the thermal shrinkage level (2). As a result, natural collagen can be chemically and physically treated to form soluble gelatins which can then be swelled through the introduction of acids to open the intermolecular matrix.

The two broad categories of collagen are fibrillar and non-fibrillar. Fibrillar collagens are defined by the presence of collagen fibers. These fibers begin as collagen molecules which covalently bond to each other to form fibrils. This occurs naturally in the body as the molecules accumulate spontaneously under physiological pH,

temperature and ionic strength. These fibrils then arrange in a "head to tail" arrangement with some overlap with adjacent collagen molecules. Figure 1.3 shows this "head to tail" arrangement with overlap. The fibrils can pack together to also form fibril bundles or fibers which have increased mechanical properties, especially for tensile applications such as tendons (6). Non-fibrillar collagens are not as varied as the fibrillar form and are mainly a constituent of the basement membrane that helps to separate epithelial tissues from mesodermal tissues. The non-fibrillar type does not form fibrils and is mainly nonhelical (1). As most of the collagens in the body are of the fibrillar type, they will be the only ones considered for the remainder of this investigation.

As subsets of these two broad categories, collagen is broken down into its more specific types based on function or location within the body. Table 1.2 shows the various types of collagen and their locations within the body (6). Of the fibrillar collagens, the most abundant is type I collagen which can be found in skin, tendon, and bone. These have relatively larger fiber diameters which are necessary to perform collagen's role in creating structure. The collagen molecule is approximately 280 to 300 nm in length. The three polypeptide chains have approximately 1000 amino acid residues each. The diameter of the collagen molecule is 1.4 nm. The central or main helical region of the fibrils that make up the collagen molecule are comprised mainly of non-polar residues with short side chains. As stated before, the high and regular glycine content allows for the close packing of this helical region. The ends of the fibril are comprised of polar amino acids with longer side chains. This arrangement allows them to bind to heavy metal ions. In the past, researchers saw striations under electron micrographs where the

Table 1.2 Collagen types and locations within the body.

Collagen Types	Location In Body
I	Bone, Tendon, Skin, etc.
II	Int. Disc, Vit. Body of Eye, Cartilage
III	Skin, Aorta, Lung, etc.
IV	Lens Capsule, Glomerulus, Basement Membranes
V	Bone, Tendon, Blood Vessel
VI	Blood Vessel, Intima Placenta, Calf Skin
VII	Chorioamniotic Membranes
VIII	Endothelium
IX	Cartilage, Cornea, Retina
X	Thoracic Cartilage
XI	Cartilage
XII	Cartilage

Source: Jain, M., P.H.D. Thesis: Micromechanical Properties of Collagen. Biomed. Eng. Dept., Rutgers, The State University, N.J., 1-23, 1989.

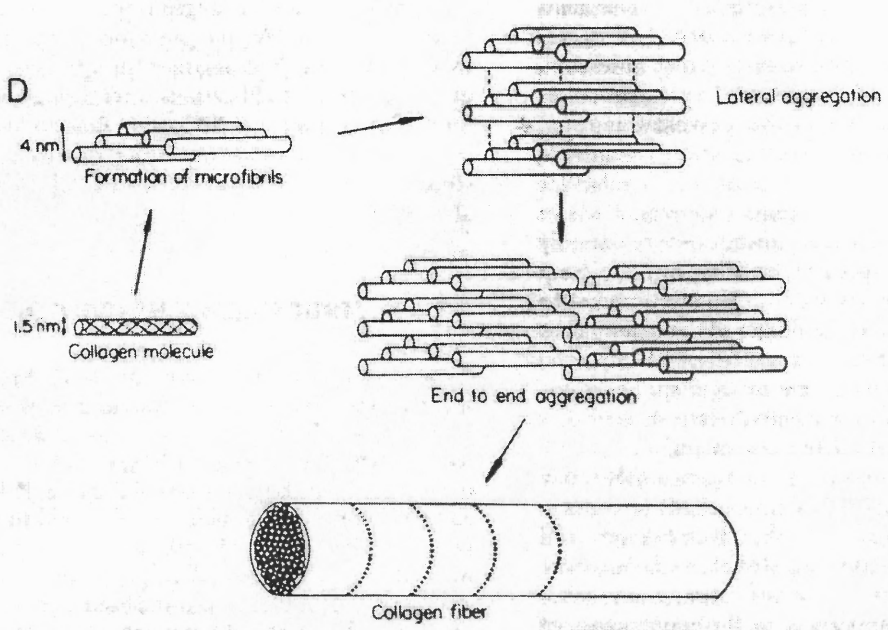

Figure 1.3 Head to Tail arrangement of microfibrils forming the single collagen fiber. Source: Rattner, Buddy et al. Biomaterials Science, Academic Press, N.Y., 84-92, 287-288, 1996.

chemical stains would bond to these nonpolar regions at set intervals of 67 nm and this allowed them to deduce the structure of the collagen fibril. Therefore, with 67 nm fibrils arranged together, the collagen molecule of 280-300 nm would be comprised of 4 fibrils which are overlapped or staggered at approximately 30 nm. Each type I collagen molecule is comprised of two arrangements of collagen chains (fibrils), the α1(I) and the α2(I) which differ in their terminal telopeptide regions. Specifically, there are two α1(I) chains which combine with one α2(I) chains to make the triple-helix. The difference comes in the number of amino acid residues for each end of the chains. For the α1(I) chain, there are 16-17 residues on the amino end and 25 residues on the carboxyl end. The α2(I) chain has 9-11 residues on the amino end with 6-8 residues on the carboxyl end. These telopeptide regions are the site for cross-linking. With cross-linking, the denaturation temperature for a collagen molecule would change from 40° C to greater than 60° C (5).

The other major or "classical" collagens are type II, III, and IV. Cartilage collagen is mainly type II. A major portion of blood vessel walls is type III collagen as well as some contamination in the skin. In general, the type II collagens are thin and the type III are intermediate sized and help provide structure and limit tissue deformation when a load is applied. Type IV collagen is the non-fibrillar variety which makes up the separation layer in the basement membrane. These are mainly sheets of collagen molecules. The remainder of the collagen types are used by the body for various functions, primarily structural support or mineralization of tissues (6). Table 1.3 shows, in general, the difference of composition between various types of collagen (7, 20).

Table 1.3 Composition of Collagen types.

Collagen Type	Composition	Supermolecular Structure
I	Low Hydroxylysine, Low Carbohydrate, Broad Fibrils	67 nm Banded Fibrils
II	High Hydroxylysine, High Carbohydrate, Thin Fibrils	Small 67 nm Banded Fibrils
III	High Hydroxylysine, Low Carbohydrate, High Hydroxyproline	Small 67 nm Banded Fibrils
IV	High Hydroxylysine, High Carbohydrate	Non-Fibrillar Network
V	High Hydroxylysine, High Carbohydrate	Small Fibers

Source: Rawn, J.D., Protein conformation and function in Biochemistry, Neil Patterson Publishers, N.C., 86-93, 1989.

1.2 Importance of Collagen as a Biomaterial

An important aspect of biomedical applications is to make the intended implant or device as biocompatible as possible. Biocompatability is defined as the "ability of a material to perform with an appropriate host response in a specific application" (1). In order for an implant to be as biocompatible as possible, certain materials are often chosen because they do not illicit a harmful response from the body. The definition applies for the lifetime of the implant, therefore if an implant is to be placed permanently into the body, it must never illicit a harmful response. Likewise, a degradable implant must not illicit a harmful response during its time of operation or after it has degraded into byproducts. Many materials are carcinogenic and others often cause clotting or encapsulation. Natural polymers can be more effective than synthetic ones because they are very similar and often identical to the items that are being replaced or augmented. The body therefore may not deem them foreign and an undesirable host response may be avoided. This can avoid the most common problems of toxicity or the inflammatory reaction. A second advantage of a natural material is that it can perform the same tasks on the molecular level as the original as well as the intended function. There is always a chance of immunogenicity of

any natural polymer, however, which increases the chance of antibiotic attack on the implant. The immunological response of the body is directed at target sites on the implant proteins. The body can produce antibodies or lymphocytes which attach to the surface of the implant leading to its degradation. In order to counter this, these antigenic determinant sites on the protein can be modified chemically. Table 1.4 shows some natural polymers and their general properties (1).

Table 1.4 Natural polymer examples and functions in host animal.

Polymer	**Incidence**	**Physiological Function**
Silk	Synthesized by Arthropods	Protective Cocoon
Keratin	Hair	Thermal Insulation
Collagen	Connective Tissues	Mechanical Support
Gelatin	Partly Amorphous Collagen	(Industrial Product)
Fibrinogen	Blood	Blood Clotting
Elastin	Neck Ligament	Mechanical Support
Actin	Muscle	Contraction, Motility
Myosin	Muscle	Contraction, Motility

Source: Rattner, Buddy et al. Biomaterials Science, Academic Press, N.Y., 84-92, 287-288, 1996.

Collagen is an example of a natural biopolymer which can be shaped for various applications. Its physical, chemical, and biological properties make it an excellent choice for a biomaterial which is also biocompatible. Table 1.5 shows some of the advantages of using collagen as a biomaterial (6).

Table 1.5 Properties of collagen which make it a favorable biomaterial.

Type of Property	**Property**
Physical-Mechanical	High Tensile Strength Low Extensibility Orientation of Fibers
Physical-Chemical	Controllable Cross-Linking by Tanning (Affects Solubility, Swelling, Resorption) Ion Exchanger Function Semipermeability of Membrane
Biological	Low Antigenicity Effect on Wound Healing/Blood Clotting

Source: Whyne, C., M.S. Thesis: Evaluation of Crosslinking Methods and Characterization of Surface Features of a Collagen-Based Dermal Equivalent. Biomed. Eng. Dept., Rutgers, The State University, N.J., 1-16, 1984.

An added advantage that makes collagen an excellent choice for an implantable biomaterial is the relative similarity among species. Due to collagen's relative standard Gly-X-Y arrangement, species differences among mammals are small (3). The triple helix configuration does not allow for major substitutions of amino acids between the species as other proteins do, making collagen a relatively constant structure (1). As a result, the collagen from other species, mainly bovine type I collagen, can be harvested for use in biomedical applications. The relatively high amounts of bovine collagen available make it an excellent source of collagen for medical applications after chemical treatment. The collagens are generally considered weak immunogens in comparison to most proteins, which may be due to a lack of tyrosine residues (8). According to some research, tyrosine had a 1.2% contribution per residue to the antigenicity of a protein. This data suggests that most of the antigenic determinants are of the steric conformation in which tyrosine is frequently involved as immunodominant amino acids (9). The use of bovine collagen in humans may lead to an antigenic response, however, due to the minor differences in the collagen amino acid sequences and the nonhelical telopeptide region (1). In order to make them less antigenic, collagen is often treated chemically. The use of glutaraldehyde has been shown to be effective in reducing collagen's antigenicity (1). As a result of exposure to glutaraldehyde, the antigenicity is reduced and will allow xenografts to be more accepted in humans without serious immunological response. Figure 1.4 shows the suspected regions of antigenic determinants (5).

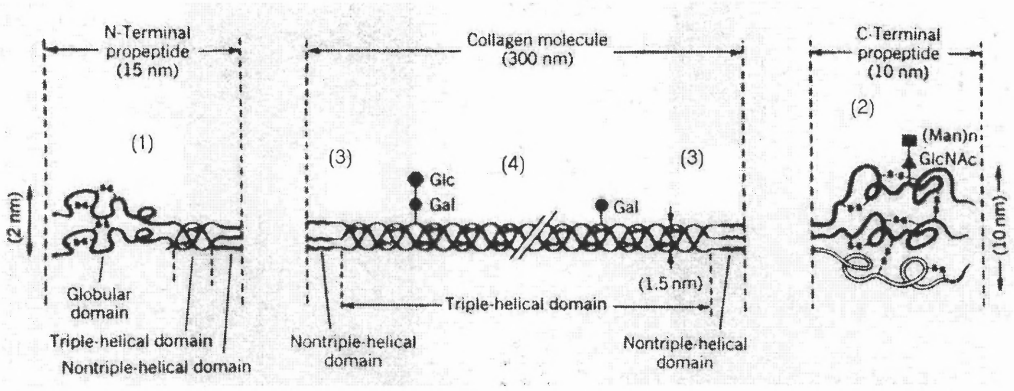

Figure 1.4 Possible antigenic regions on the collagen and procollagen molecule. (1) represents the amino propeptide, (2) represents the carboxy propeptide, (3) shows the amino and carboxy telopeptide regions, and (4) represents the main triple-helical region which can be antingenic.
Sources: Kroschwitz, J., Collagen in Encyclopedia of Polymer Science and Engineering, Volume 3, Wiley Interscience Publishers, N.Y., 699-725, 1985. Mayne, R., Burgeson, R., Structure and Function of Collagen Types, Academic Press, N.Y., 1-36, 1987.

Depending on the intended application, the ability for natural polymers to be broken down by enzymes allows for the complete degradation of an implanted material. This can be an advantage if the implant is only meant for short-term usage and eventual replacement by the body's own materials. For collagen, the cells can synthesize new collagen which normally forms a new architectural arrangement, such as scar tissue, in wounds. This is one step in the wound healing process that the body begins as a result of damage caused by implantation.

This degradation can also be a disadvantage if these enzymes destroy the implant before it completes its intended task. Collagen is susceptible to attack by collagenases in a physiological setting. These collagenases are present in healing wounds and are a primary reason for the degradation of collagen implants. Luckily, through various physical or chemical methods, the degradation rate of collagen implants can be controlled.

In order to make the material more survivable in the body, collagen can be modified by several physical means. The most common physical method is dehydrothermal treatment. By heating in an oven, collagen can be severely dehydrated which creates interchain amide links. By exposure to temperatures in excess of 105° C with atmospheric pressure for a few hours, the collagen can produce cross-links which help prevent degradation of the helix. The ultimate tensile strength may be improved by preventing interfibrillar slippage and also removing the water molecules which swell the matrix and prevent hydrogen and other forms of electrostatic bonding between the collagen molecules (10). Dehydrothermal treatment of collagen requires a careful balance between the amount of time exposed to heat to provide adequate cross-links and the amount of time which could lead to the denaturing or degrading of the tissue (11). Another less widely used method for cross-linking collagen is through exposure to short wave (254 nm) ultraviolet irradiation or gamma radiation (11,12). An issue with this, however, is in determining how deep the radiation will penetrate and subsequently how many cross-links it will produce. Although these methods do not introduce potentially harmful chemicals to the collagen, they are not as effective as chemical treatments which have been used commercially for years and, as previously stated, can help lower antigenicity while increasing the tensile strength of the collagen.

The more prevalent method of cross-linking is through chemical treatments. The most common chemical method for introducing cross-links to reconstituted collagen is through the use of glutaraldehyde, the same chemical which helps reduce antigenicity. The leather industry has used dialdehydes in the past as tanning agents, and laboratories have used them as fixatives for histological studies. Glutaraldehyde has been recognized

as an effective chemical method for increasing the cross-link density. This allows implants to remain patent for extended periods of time before degradation of the implant collagen. The implants can survive for periods of a few days to several weeks, depending on the amount of cross-linking (1). Glutaraldehyde cross-linking is not only more resistant to bioattack, but also shows better blood compatibility which decreases the chance of causing a clot in vascular applications. Glutaraldehyde induces inter-chain cross-links by a suspected linkage of two lysine side chains with two molecules of glutaraldehyde as seen in figure 1.5 (1). By increasing the concentration of the glutaraldehyde, it is possible to increase the number of cross-linked sites per gram while also creating a higher cross-link density deeper in the fibers. Since glutaraldehyde is also known to penetrate slowly, there can be a problem of trying to fix larger or thicker walled implants (13). A second problem is the prevention of further fixative penetration deeper into the implant once the outer layer is cross-linked sufficiently enough to stop absorption

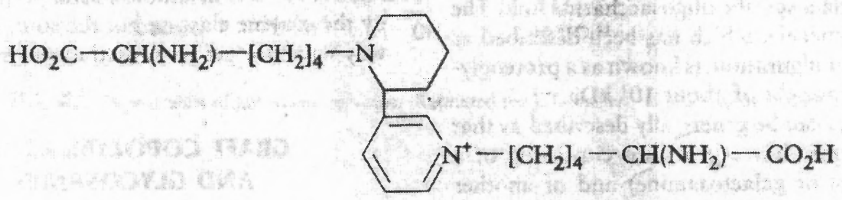

Figure 1.5 Suspected glutaraldehyde cross-link in which two lysine side chains are bonded with two molecules of glutaraldehyde. The complexity of glutaraldehyde has made the nature of cross-links controversial and this is only one possibility.
Source: Rattner, Buddy et al. Biomaterials Science, Academic Press, N.Y., 84-92, 287-288, 1996.

of the glutaraldehyde (11,14). Applications of thin walled tubes as used in vascular implants or thin films such as skin replacements avoid such a problem with fixative penetration. Unfortunately, the amount of cross-linking will also cause the material to become more brittle. A careful balance between the brittleness and the amount of cross-linking needed for the correct mechanical properties and degradation time must be determined (15).

1.3 Applications of Collagen Tubing

The possibilities for collagen tubes in biological applications are varied. Hypothetically, any hollow tube application in the body can be replaced with a collagen tube if it had the right properties to mimic the original without illiciting a negative host response. The most promising of these applications are vascular replacements or grafts. The history of the venous autograft dates back to 1949. The patient's own saphenous vein is usually removed from the calf for use in other areas of the body, primarily for heart bypasses or for below the knee arterial surgery. The obvious problem with this is that there are only two saphenous veins, one in each leg, and their removal will affect the blood flow through the leg. The other issue is that 20% - 30% of patients needing bypass have an unsuitable saphenous vein to be used for surgery. The saphenous vein could be too small or unusable due to some disorder such as phlebitis or varicosities (1). There is always a possibility of failure due to thrombosis or neointimal hyperplasia which clots the graft making it unusable. If the autologous saphenous vein becomes occluded after implantation, another one must be found in the body or alternative must be found.

Besides the autologous saphenous vein, other sources are homografts, which are veins from other humans, xenografts, which are from animal sources, and synthetic grafts, which are manufactured mainly from polymers that are foreign to the body. Homografts have high failure rates due primarily to antigenicity. Xenografts are also susceptible to thrombosis and rupture. In both cases, chemical treatment by glutaraldehyde has been shown to reduce antigenicity. Unfortunately, these must still be harvested which means that a suitable vein must be found in a donor human or animal.

Although synthetic vascular replacements can be mass produced, there is always a chance that the body will reject the foreign material and try to destroy it or that the material will cause a damaging reaction within the body, especially with blood (1). The most common synthetic graft used today is made of PET (polyethylene terephthalate) commonly known as Dacron™ for sites greater then 4 mm in diameter. Another promising polymer is ePTFE (expanded poly(tetrafluoroethylene)) commonly known as Goretex™ which has the tensile strength necessary as well as low probability of occlusion (1). The biggest issue with synthetic polymers is that they are unsuitable for use in grafts with less than 4 mm inner diameter (1). This makes them unusable for bypass or reconstructive procedures below the knee or in cardiovascular arteries. These problems may arise due to the slower flow in small diameter blood vessels which allow for increased contact time with the polymer. Another possibility is the increased surface to volume ratio which leads to higher rate of activation of blood coagulation including complement, platelet, and other pathways which eventually lead to occlusion of the implant (1). What commercial graft manufacturers sometimes do is pre-clot the implant using the patient's blood in order to make the polymer impervious to leakage while

making it more recognizable to the body. Collagen and fibroblasts from the host will eventually replace this blood clot. In order to shorten the process, some manufacturers put collagen into the graft instead of using the patient's blood. The collagen is then replaced naturally by the body without the need for pre-clotting with patient's blood (1).

The question now becomes, if there is no suitable saphenous vein located, and other sources prove unusable, where will the graft come from for this patient? A logical solution is to use the biopolymer collagen shaped into a tube and treated either physically or chemically that has been manufactured for such a purpose. Collagen tubes have already been tested for use as nerve conduits for repair of damaged nerves. In these studies, the two nerve ends were either held within a collagen tube without touching the two ends or after touching the two ends in order to act as a conduit which could lead to nerve regeneration (16). They have become a common device for use in nerve repair experiments.

Collagen tubes have also been used in vascular applications for support as well as artery and vein replacement. In one hypothetical usage, a collagen tube was used around a venous graft in order to give added support. The collagen tube apparently preserved the contractile function of the graft without causing a change in flow rate or blood pressure. Collagen's low antigenicity has been utilized to make synthetic grafts more biocompatible and minimize some of the complications with clotting and encapsulation which can destroy the effectiveness of the implant.

These extruded collagen tubes can be considered as short fiber-reinforced tubes due to the fibrillar components supporting the main collagen matrix. As such, a basic look at what can be achieved or what possible changes the fiber reinforcement have on

the properties would help determine the possibilities of these collagen tubes. In industry, composite materials are created with fibers of high strength being embedded in or bonded to a matrix at set intervals. In this way the fibers and matrix keep their own physical and chemical identities but will have a combination of properties that are unattainable individually (17). The fibers will act as the load-carrying members while the matrix holds them in place. In order to optimize the arrangement of the fibers in the matrix, the fibers are often wound around the tube over a mandrel. Another method is to embed the fibers during extrusion through a die. Figure 1.6 shows two dies, a classical version which gives basic orientation of the fibers along the pipe axis, and a diverging die which is able to orient the fibers in the hoop direction which will help tubes that are under severe hoop stresses from failing (18). The classical die is similar to that used in this study to extrude and orient the collagen onto guide rods giving them a certain longitudinal angle which can contribute to change properties.

The winding angle helps determine the strength and deformation in composite tubes. Table 1.6 shows some experimental data found in an unrelated study on the difference of elastic modulus and Poisson's ratio in E-glass fiber reinforced epoxy resin tubes (19). The numbers from this section of the experimental data suggest that the winding angle is able to change the elastic modulus of a material and that in tension, the higher angle doesn't perform as well as something around 45° or the optimum value they obtained of 55°. The study also showed, however, that in burst tests, the higher angle attained a larger elastic modulus which could prevent rupture, which translates to the necessity of a balance between the ability to stretch in tension and also radially to prevent bursting. With this information as a basis, it seems logical that the collagen tubes, which

are self-reinforced due to the fibers supporting the tube matrix, can be affected by the rotation angle at which the material is deposited by semi-orienting the fibers.

Table1.6 Experimental data which shows the influence of rotation angle on elastic modulus.

Angle	Elastic Modulus (Gpa) Tension	Poisson's Ratio	Elastic Modulus (GPa) Burst	Poisson's Ratio
+/- 55°	18.70	0.309	25.98	0.550
+/- 75°	13.86	0.136	40.50	0.424
+/- 45°	16.54	0.454	15.61	0.459

Source: Soden, P.D., Kitching, R., Tse, P.C. & Tsavalas, Y., Influence of Winding Angle on the Strength and Deformation of Filament-Wound Composite Tubes Subjected to Uniaxial and Biaxial Loads, *Compos Sci and Tech*, 46, 363-378, 1993.

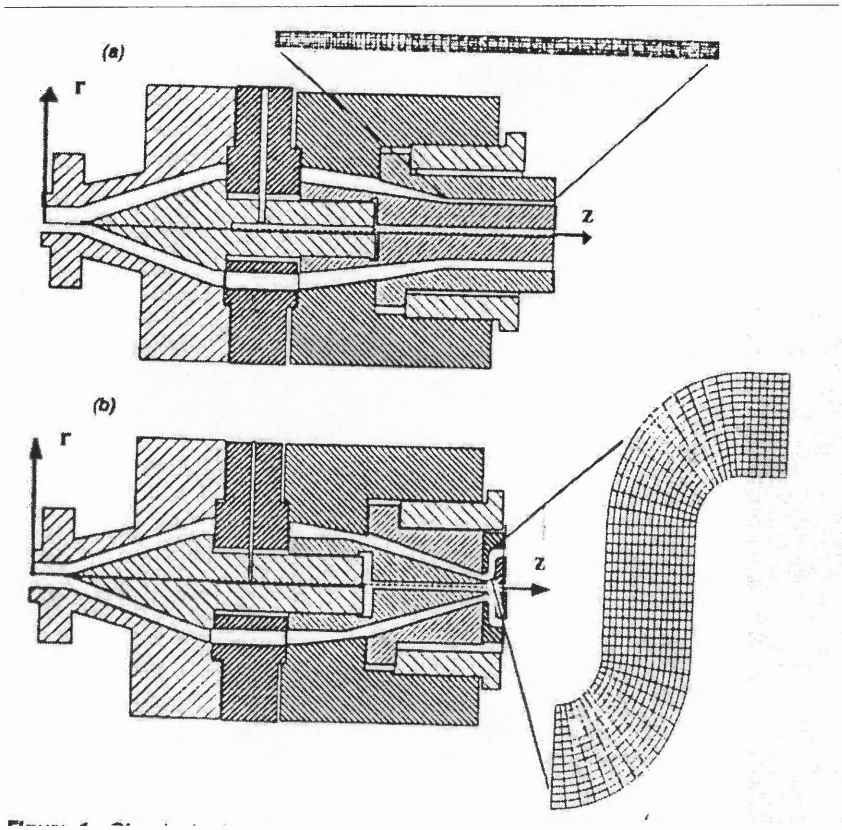

Figure 1.6 Two types of extrusion dies. Top is the classical which resembles the extrusion method used in the present study. The lower die is an example of a diverging die which could be useful in future collagen tube research. Source: Ausias, G., Vincent, M., Optimization of the Extrusion Process for Glass-Fiber-Reinforced Tubes, *Jour Thermoplastic Comp Mater*, 8, 435-448, 1995.

CHAPTER 2

MATERIALS AND EXPERIMENTAL METHODS

The collagen used to create the tubes for this experiment was donated by Nitta Casing, Inc, Somerville, N.J. This collagen had been extracted from fresh, uncured bovine hides. Using a similar procedure as outlined by Komanowsky et al. (20), the collagen hides were limed, dehaired, split, and chopped into small pieces which were subsequently swollen with acid. The collagen was precipitated from this aqueous solution and finally lyophilized. This swollen collagen gel was received from the Nitta Casing company and stored in a refrigerator at 4° C as recommended by the supplier.

Nitta Casings, formerly Devro Inc, supplied similar collagen for experimentation which was characterized in 1983 by Weadock (21) by SDS (sodium dodecyl sulfate) polyacrylamide gel electrophoresis. The material was characterized as typical type I collagen without noncollagenous contamination by protein. Whyne, using the same collagen samples, had an amino acid assay performed by the Connective Tissue Laboratory (University City Science Center, Philadelphia, Pa.) and obtained the amino acid content of the collagen (22). He concluded that the collagen from Nitta closely resembled that of animal type I collagen when compared to that found by Kuhn (23).

The collagen tubes were extruded using a special collagen extrusion machine developed by ZOKO spol. S r.o. of Czechloslovakia. The collagen machine used a piston to force the collagen gel through a rotating mandrel where it was deposited on a guide rod. The rod itself was lifted away from the mandrel to form an even coating. The rod can then be removed to form a collagen tube. The collagen was deposited onto the rod after passing through a rotating head which oriented the gel to the left or the right. The rotation

head had speeds ranging from 22 – 260 rpm in either direction. In order to adjust the thickness of the tube, the pulling device also had variable speeds ranging from 152 – 1522 mm/min in the upward or downward direction. The rate of extrusion wass also adjustable by controlling the motion of the piston or dosing head. The dosing head ranges from 0.5 to 6.8 mm/min with a rapid motion option of 3.9 m/min if necessary. The collagen machine had a cylinder with a volume of approximately 1965625 mm^3 or 1965.625 cc. For each trial, the cylinder was only filled approximately ¾ full and was refilled after running every four tubes. The maximum pressure allowed in the cylinder head was 3 Mpa and was regulated by an electronic meter attached to an oil reservoir which shut off the extrusion if the pressure exceeded the maximum value. To allow for chemical treatment of the tubes, homemade baths were made from PVC piping 40 in. (101.6 cm) long and sealed on both ends with caps adding an additional 1 in. (2.54 cm) length. These baths were then cut in half lengthwise to provide adequate length and ease of access.

2.1 Extrusion Process

2.1.1 Protocol for Pre-extrusion

One of the PVC baths was filled with 99% pure Glycerine from Fisher Scientific Company of Somerville, New Jersey. The stainless steel rods, 36 in. (91.44 cm) in length, were placed into the glycerine bath and allowed to soak for about 10 minutes providing a coating to the rods. The guide rods were then removed and hung to allow excess glycerine to drain off back into the glycerine bath.

2.1.2 Protocol for Extrusion

After turning the machine on and allowing it to warm up, the piston was lowered to its lowest point and the piston head was manually pushed into place at the bottom of the cylinder. Collagen was then hand packed tightly into the cylinder until it was approximately ¾ full. The desired extrusion head and nozzle were attached to the machine after ensuring the guide rod would fit through the nozzle without any interference. The nozzle used was 3/16 in. (0.476 cm) in diameter and the extrusion head was 3/8 in. (0.953 cm) in diameter. The cylinder was then sealed and the tube from the cylinder head was run into the extrusion head manifold. The swinging arm was closed so that it sat directly over the extrusion head. A coated stainless steel rod was taken from the hanging rack and inserted through the bottom of the nozzle up through the extrusion head and then clamped into the swinging arm. The machine settings were then entered for the desired extrusion rate, rotation speed, and linear pull speed. In order to ensure no stoppage of the tightly packed collagen, the extrusion was started and collagen filled the tube from the cylinder to the extrusion head manifold.

Once the collagen began filling the manifold, the rotation motor was started. The collagen was continuously filling the manifold and finally became visible around the rod through the top of the extrusion head. At this point, the linear drawing arm was then activated and moved at the desired speed. The collagen was now being extruded onto the rod and a visual check was made to detect for gaps in the tubes. Once the guide rod had completely entered the manifold, the extrusion and rotation was stopped to prevent wasting of collagen. The swinging arm was allowed to rise until the guide rod was

completely clear of the manifold at which point the arm was opened and lowered. The rod was removed and hung on the drying racks.

This process was repeated for each of the tubes with only minor changes to the settings when necessary. After four tubes, however, the cylinder was refilled with collagen to prevent gaps from forming in the tubes. After each trial was finished, the rods were taken for post-extrusion treatment and the machine was cleaned.

2.1.3 Protocol for Post-extrusion Tube Treatment

The post-extrusion process was primarily concerned with chemically treating the collagen and drying the tubes for removal from the guide rods. Under advisement from Dr. Salvatore Romano and various a 1% ammonium hydroxide solution was used for coagulation of the collagen with a 5 % glutaraldehyde solution used for cross-linking. In order to ensure adequate chemical concentrations for all the tubes, these chemicals were refilled after every four tubes with the remainder of the chemicals being removed for disposal.

Using exclusive baths, 1 liter of glutaraldehyde and 1 liter of ammonium hydroxide were prepared for treatment of the tubes under a ventilation hood. The first stainless steel rod was removed from the hanging rack and immersed completely in the ammonium hydroxide solution. The tube soaked for 10 minutes with occasional agitation and rotation of the rod to ensure good chemical absorbance. After the 10 minutes had elapsed, the rod was removed from the bath and washed under running water to remove any excess chemical that may have accumulated on the surface. The collagen was then washed for 2 to 3 minutes under running water.

After the washing, the rod was immersed completely in the glutaraldehyde solution bath and allowed to soak for 5 minutes with occasional agitation and rotation. After the 5 minute treatment, the collagen was removed from the glutaraldehyde and washed under running water for 2 to 3 minutes. The rod was subsequently hung on the vertical hanging rack to allow excess moisture to drip off as the tube dried.

The procedure was repeated for the remaining samples. After every four tubes, however, the chemicals were replaced by pouring the old chemical into a chemical safe disposal container and filling the bath with another liter of ammonium hydroxide and glutaraldehyde. Stainless steel rods with collagen tubes were left to dry under no special atmospheric conditions for 18 to 24 hours. The tubes were examined visually to determine if adequate drying had occurred on the surface by looking for moist gellatenous areas.

Once all the tubes of the trial were deemed dry, four baths were filled with water and prepared to hold the rods. Each bath held 2 rods, the 2 rods which corresponded to the same rotation speed. The collagen was immersed completely in the water baths in order to rehydrate the tubes. Rehydration time was set tentatively for 1 hour and 30 minutes to allow enough water to absorb through the entire tube. At this point, the tubes were cut to the desired length and slipped off of the stainless steel rods. The rehydration made the collagen tubes more flexible and with slight twists at small intervals along the tube, the bond with the rod was loosened enough to pull the cut tubes off smoothly without damaging the tube or causing it to lose its shape. Some of the rods were not completely rehydrated under the standard time, particularly the thick set of tubes, so they were returned to the water bath for an additional 30 minutes until they were easily slipped

off of the stainless steel rods. The free tubes were examined to determine if there was major damage, i.e. void areas or gaps. In total, 3 tube samples were cut from each rod each being 6 in. (15.24 cm) for a total of 6 samples in each rotation rate and 24 samples total for each trial.

With the tubes no longer supported by the stainless steel guide rod, curling would occur with the final drying without intervention. To prevent his undesirable shape change, the collagen tubes were placed in drying racks made from cardboard. A screw of the same diameter as the guide rod was placed in each end of the tube before the tube was laid onto the cardboard rack. The two ends were then held down with clamps at the site of the screw to prevent the drying tube from slipping out and curling. The clamps had to be secured tightly due to collagen's tendency to shrink while drying. In order to prevent the curling from occurring in the direction away from the cardboard, a piece of corrugated cardboard was placed over top of the collagen tube. This also prevented major side motion. Light weights, approximately 5 grams, were placed on the top layer of cardboard between adjacent tubes to prevent the drying tubes from lifting the cardboard off as they dried. The tubes were allowed to dry for an additional 18 to 24 hours and were then examined to determine damage, major curling or shape changes as well as complete drying before being removed from the rack. The finished tubes were now labeled and ready for testing.

Table 2.1 shows the criteria for each trial and outlines the rotation rate values and the linear draw speeds which were utilized for the tubes in each trial. The extrusion rate was not varied and was set at $50cm^2$ / min. Figure 2.1 shows the general protocol for the extrusion of tubes and the tests performed.

Table 2.1 Trial and tube classification with values on rotation rate and linear draw rate.

Linear Draw Rate **(mm/min)**	Trial # - Rod Number, Tube Letters			
High (1270)	2 – 1 a,b,c 2 a,b,c	2 – 3 a,b,c 4 a,b,c	2 – 5 a,b,c 6 a,b,c	2 – 7 a,b,c 8 a,b,c
Medium (743)	1 – 1 a,b,c 2 a,b,c	1 – 3 a,b,c 4 a,b,c	1 – 5 a,b,c 6 a,b,c	1 – 7 a,b,c 8 a,b,c
Low (383)	3 – 1 a,b,c 2 a,b,c	3 – 3 a,b,c 4 a,b,c	3 – 5 a,b,c 6 a,b,c	3 – 7 a,b,c 8 a,b,c
	None (0)	Low (58)	Medium (130)	High (260)
	Rotation Rate (rpm)			

(Note: Extrusion rate was left constant with a value of 50 cm^2 / min)

Figure 2.1 Outline of General Protocol

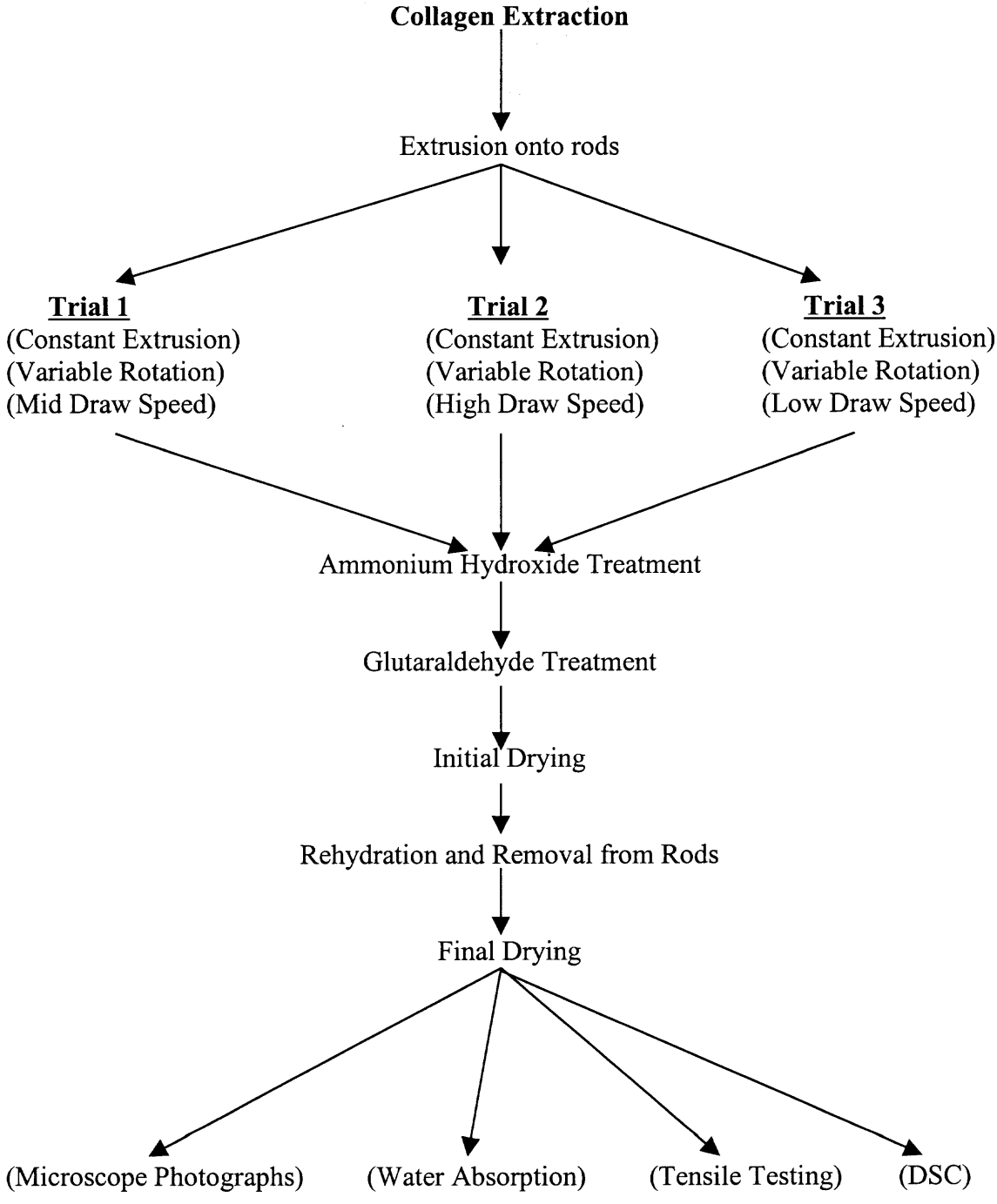

2.2 Protocol for Microscopic Photographs

2.2.1 Sample Preparation

Sections were cut out of the side of collagen rods which had undergone low rotation rate and were slightly moistened using tap water. The sections were then placed with the interior of the tube facing upward on a standard slide and a cover was placed on top with a weight to flatten out the tube section. The same procedure was repeated on separate slides with the exterior of the tube facing upward.

Pure collagen smears utilized the gelatenous untreated and unextruded collagen for slide preparation. A small amount of collagen was placed onto the slide and a cover was applied with pressure to flatten out the collagen.

2.2.2 Photographs

The slides were examined using a Zeiss microscope with camera attachment. The camera used standard 35mm film with a shutter speed of 200. The first slide examined was to calibrate length at various magnifications using a specialized side. Photographs were taken of this slide at 25x, 63x, and 100x magnifications which were the only objectives available on the microscope.

The pure collagen smears were studied under each of the magnifications using both regular and polarized light. Photographs were taken at each magnification of areas which showed a large number of fibers to allow for measurement. Polarized light photographs were also taken at the same locations to examine the fiber boundaries.

The sample tubes were examined next and photographs of the interiors were taken using the three magnifications available. In general, due to the consistency of the

appearance of these photographs as far as fibers being visible throughout the matrix, it was decided to only photograph the exterior tube samples at the medium magnification of 63x as representative of the surface appearance. All photographs were then developed and the fibers were measured to get values for the lengths and diameters for the various samples.

2.3 Protocol for Water Absorption Test

2.3.1 Sample Preparation

A selection of tubes from each rotation rate and each trial were taken and cut into 4 cm lengths. Four cups were used as baths and were prepared using regular tap water in room temperature. The cut samples were massed and measured before the experiment to determine the dry mass and dimensions. The samples were then labeled with rotation rate and trial number for identification.

2.3.2 Water Absorption Study

The samples were placed into the water baths and the allowed to soak in water for one full hour. After the desired time had elapsed, the samples were removed from the water bath and water that had accumulated inside the tube was removed via paper towel as well as any excess surface water. The mass and dimensions of the tube were once again measured and all the values were recorded for analysis.

2.4 Protocol for Instron Tensile Testing

2.4.1 Sample Preparation

One tube from each of the four rotation categories was chosen in each of the three trials for a total of 12 samples. The ends were removed from the samples so that only the middle section would be tested to prevent possible defects from the drying process to affect the data. Samples were cut to 4 in. (10.16 cm) to allow for a 2 in. (5.08 cm) gap with 1 in. (2.54 cm) firmly secured in the holding clamps on each end. The samples were left in a dry state and had wooden plugs fitted into each end prior to testing. The wooden plugs were fashioned to fit snugly into the ends of the tube and were meant to give support to prevent the tensile clamps from collapsing the tube.

2.4.2 Machine Preparation

Tensile testing was done on a Tinius Olsen tensile tester which had been calibrated on 2/3/00 by Dr. Victor Tan. The machine was calibrated daily using fine movement adjustments and left on so that internal circuits did not have to reset and re-calibrate, a process which would take 4 hours to complete. Two load cells were utilized depending on the thickness of the sample, the 100 lb load cell for the thin and medium tubes and the 1000 lb load cell for the thickest tubes. A built in recording device allowed the machine to record the force versus displacement curve which could be analyzed with minor calculations.

2.4.3 Tensile Test Trials

After calibrating the machine, the clamps were opened and a sample was placed into top clamp and sealed. The gap between clamps was set to a distance of 2 in. (5.08 cm) which allowed for 1 in. (2.54 cm) of tube, with wooden plug, to fit into each clamp. Due to the difference in thickness of tubes between the three trials, this gap was set using fine motion adjustments before each test began. The bottom clamp was closed, and the gap distance was measured. If the gap was too large or small, the bottom clamp was re-opened and adjustments were made on the machine until the closed clamps were the correct distance apart.

For all trials, the pulling speed was set to 0.5 in/min (1.27 cm/min). The settings for load cell and the recording device were adjusted to the specific trial being run. The thin tubes and medium thickness tubes both utilized the 100 lb load cell. For the thin tubes, the data recorder was optimized for 50 lb. The data recorder was set to 100 lb for the medium thickness tubes. The thick tubes required a 1000 lb load cell to be used with the data recorder set to 250 lb. These data recorder optimizations were made to allow the force vs. displacement curves to have adequate size for analysis for each of the specific trials.

Once all the settings were set, the tensile test was run. The machine stretched the tubes until fracture at which point the pulling arms were stopped. The clamps were re-opened and the sample was studied to ensure the break was close to the middle region of the tube and not totally in the area held by the clamps, which could have been damaged. Any tubes that broke in this region were re-tested using another sample from the same

tube or another in the same rotation rate. The data recorder was reset and the next test began using the same protocol for mounting the sample and running of the test.

2.5 Protocol for DSC

2.5.1 Sample Preparation

Samples were cut from the edges of the selected pieces chosen for testing. Using a razor, a small portion was cut from the edge of each sample and placed into a DSC aluminum pan with a cover. The sample mass was found using a Cuhn C-30 electric microbalance calibrated for milligrams. After the mass was determined and recorded, the edges of the aluminum pan were rolled over the cover piece on top of the sample to seal the pan.

2.5.2 DSC Machine Preparation

The differential scanning calorimetry tests were performed using a Perkin Elmer DSC 7 DSC machine. The DSC apparatus was attached to a PC through an interface device that recorded the data for transmittal to the software and control of the DSC. The machine had been calibrated by Dr. Victor Tan earlier in the month, to confirm the accuracy of the DSC data. Before operation, the bin around the testing chamber was filled with ice, and gaseous nitrogen was pumped into the testing chamber. In addition to the main machine calibration, a daily baseline was obtained on each day samples were to be tested. The baseline was performed using an empty aluminum pan and cover that are identical to those used for the samples. Each sample run used this daily baseline to compare the data obtained to a blank pan thereby removing any inconsistencies of the machine and environmental factors.

2.5.3 DSC Trial 1

The initial DSC tests were set to run to a maximum temperature of 350° C from a start temperature of 20° C. The scanning rate was set to 20° C/min for all samples. The sample pan was placed into the testing chamber which was then sealed. The machine was allowed to gain control over the temperature before the trial began. As previously stated, the baseline established at the beginning of each day was used as a comparison for data collection by the interface. The test was started once temperature control was attained. Once the maximum temperature was attained, the DSC returned to the load temperature and the data was saved for analysis.

The analysis was done with the same software as the data collection and was limited to locating peaks and optimizing data ranges. The first approximately 20° C of the tests were used for equalization of data collection and were therefore either deleted or not considered in the analysis. The other ranges were optimized to try to get the same power level and temperature (Y and X respectively) ranges for all samples to allow for visual comparison between samples. Once the data had been optimized, a plot was made.

2.5.4 DSC Trial 2

Following the initial DSC trial, it was decided to run a second set which followed a different protocol. Whereas the first trial ran through the whole 350° C temperature range in one run, the second trial established an initial water removal stage to determine the difference in DSC data. The samples were prepared the same way as in trial 1 and loaded into the machine. The scanning rate was once again set to 20° C for all samples. For this trial, the samples were heated to 80° C and the machine held this temperature for 30

minutes to drive the water out of the samples. Once the 30 minutes had passed, the machine returned the temperature to 20° C. Once the temperature control had been attained, the actual test was run to 300° C. (Note: The final temperature was lowered to 300° C since degradation occurred slightly before this temperature. Allowing it to reach the higher temperature might damage the machine by leaving residues.) Once the maximum temperature was attained, the machine returned the sample to the load temperature of 20° C.

The analysis was done with the same software as the data collection and was limited to locating peaks and optimizing data ranges. In an attempt to make the data more visually comparable, the power level range (Y) and the temperature ranges (X) were set to approximately the same levels. Once the data had been optimized, a plot was made.

CHAPTER 3

RESULTS

3.1 Collagen Extrusion and Tube Formation

Collagen was successfully extruded onto the stainless steel guide rods. All three draw rates and all four rotation speeds produced wet tubing which was then chemically treated and dried as previously described. Each trial had 8 guide rods full of collagen tubing with 2 rods for each rotation rate. The full lengths were cut into 3 portions from each rod and produced 6 tubes of collagen for each rotation rate for a total of 48 tubes for each trial and 144 total tubes.

The color of the collagen tubing was yellow when compared with the original untreated collagen which was a side effect of the glutaraldehyde treatment. The thickest tubes were the darkest color, resembling a dark yellow/red color. The thinnest tubes still had a yellow color but were more translucent than the thickest and medium sized tubes. The surface of the tubes were slightly rough to the touch and all tubes were checked for gaps or breaks in the surface. The collagen tubes, post chemical treatment, were also easier to handle than comparable non-chemically treated tubes when being removed from the guide rods even when re-hydrated. This suggested that the treated collagen had some crosslinking to make the tubes feel more stable and resist breakage.

In addition, the changing rotation rates aligned the fibers of the collagen surface to various angles from the vertical. The trials were conducted with the lowest draw speed of 383 mm/min, intermediate draw speed of 743 mm/min, and most rapid draw speed of 1270 mm/min. The lowest draw speed produced the thickest tubes and the most rapid draw speed produced the thinnest tubes. The variable rotation rates were set at zero

rotation, low rotation with 58 rpm, medium rotation with 130 rpm, and high rotation with 260 rpm. The tubes with no rotation had alignment of the fibers in the longitudinal direction of the tube or 90° from the horizontal plane. The other angles had to be calculated using the rotation rates and the linear draw speed seen in the Materials and Methods section. This made the assumption that the radius was that of the guide rod even though this does not take into account the material thickness itself. This assumption was made for simplicity and the inability to measure the wet tube's radius. Table 3.1 shows the various angles of alignment measured from the transverse (horizontal) plane. The lowest angles were seen in the highest rotation since they were able to complete many revolutions before the guide rods were pulled away. The highest angles, besides the no rotation, were therefore seen in the low rotation tubes since the guide rods were being pulled away before the revolutions were completed. These angles will no doubt affect the properties seen in the various tubes.

Table 3.1 Angle of Fiber Alignment in Degrees (Angles measured from horizontal plane)

		Rotation Rate (rpm)			
		0 No	**58 Low**	**130 Medium**	**260 High**
Linear Draw Rate (mm/min)	**383 (Trial 3 Tubes)**	90°	24.58°	11.15°	5.63°
	743 (Trial 1 Tubes)	90°	40.59°	20.92°	10.82°
	1270 (Trial 2 Tubes)	90°	55.67°	33.16°	18.09°

3.2 Microscopic Photographs

Various photographs were taken of collagen tubes from each of the trials and also pure collagen smeared onto slides.

3.2.1 Pure Collagen Smear

The pure collagen smear was investigated at magnifications of 25x, 63x, and 100x. The smear under regular light (with amber hue) shows natural formed fibers varying in length and diameter and with no regular arrangement. The smear was also photographed under polarized light to help distinguish boundaries between fibers that were close to each other as well as investigate the light reflection of the fibers. Sample photos are shown in figure 3.1 for regular light at 63x magnification and figure 3.2 for polarized light at 63x magnification.

The overall examination showed that although the natural forming fibers do have different sizes, they were approximately the same length and diameter with appearances changing due to the fiber not being completely in the plane being examined or damage as a result of the preparation. Higher magnifications showed smaller fibers attaching adjacent larger fibers. These smaller fibers were 0.001 cm in diameter and lengths vary according to distance between adjacent larger fibers. Fiber length and diameters were examined more closely and table 3.2 shows the average values for the length and diameter of these pure collagen fibers. The values used were from 10 random fibers located on the photograph which were measured and then divided by the appropriate magnification to obtain the actual length and diameter. For the pure collagen the length average was 0.572mm and the diameter average was 0.0463mm.

Table 3.2 Fiber Length and Diameter of Collagen Smear and Tubes From All Trials

Sample Type	Length Average (mm)	Diameter Average (mm)
Pure Collagen Smear	0.572	0.0463
Trial 1 Tubes	0.430	0.0510
Trial 2 Tubes	0.420	0.0495
Trial 3 Tubes	0.420	0.0460

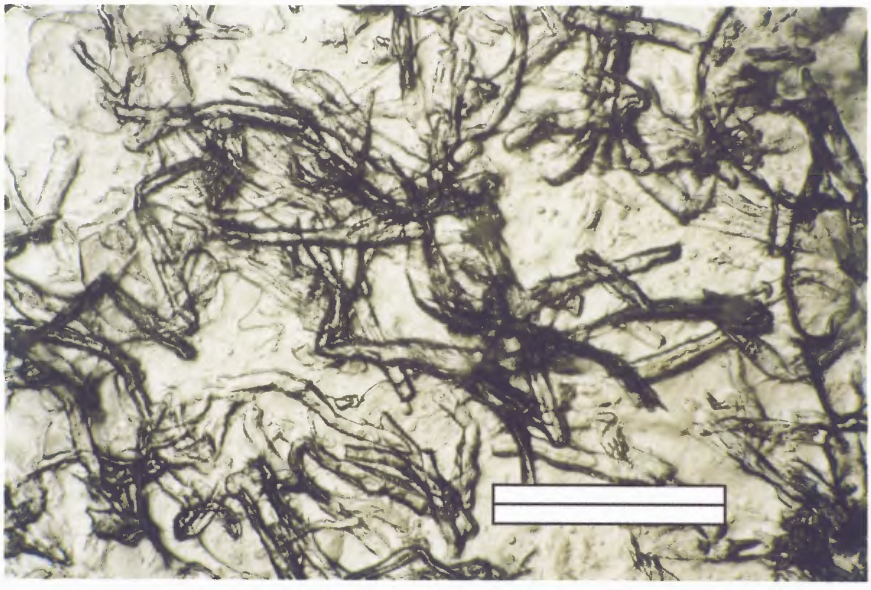

Figure 3.1 Pure collagen smear under regular light at 63x magnification. (Note: Marking is 0.5mm to show scale.)

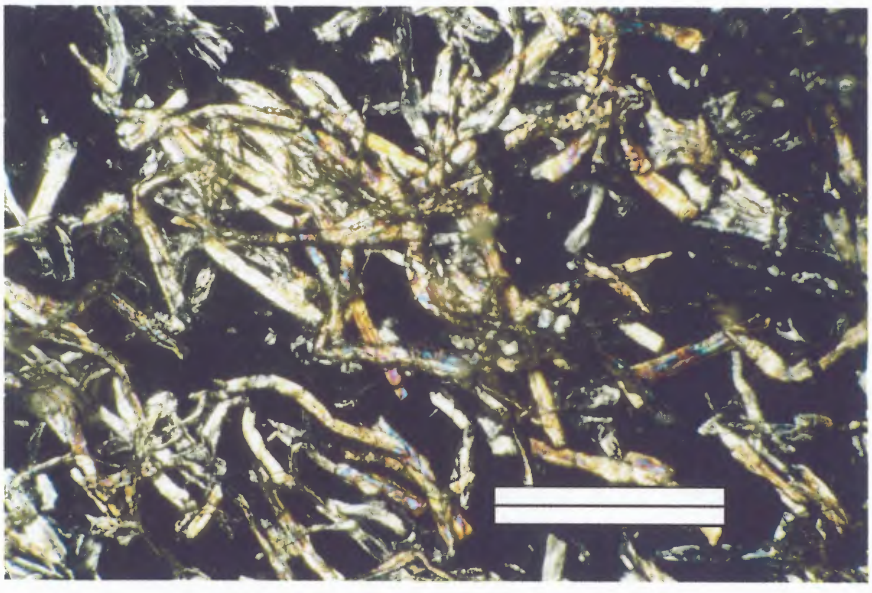

Figure 3.2 Pure collagen smear under polarized light at 63x magnification. (Note: Marking is 0.5mm to show scale.)

3.2.2 Trial 1 Tubes

The medium thickness tubes were examined here and the microscope photos showed a thick and consistent amount of material. The fibers on these interior pictures were in no regular arrangement. Under low magnification, there were no visible smaller fibers due to the background matrix material obscuring the view. Under higher magnification, however, there were smaller fiber-like projections which appeared to connect some adjacent larger fibers. There was no noticeable difference between the structure of the collagen tubes at high, medium, or low magnification. Collagen fibers were arranged in a non-linear pattern throughout the matrix, however, and were located in random planes which caused them to run through different areas of the matrix and reinforce in several planes. The fiber length and diameters were measured once again and the values appear in table 3.2. Figure 3.3 shows the trial 1 tube interior under regular light and 63x magnification.

3.2.3 Trial 2 Tubes

The trial 2 tubes were the thinnest tubes and they showed the same fiber reinforcing of the solid collagen matrix. There was no regular arrangement of the fibers on the interior surface photographs and the fibers once again are situated in various planes of the structure. There was no noticeable difference between the arrangement of fibers between the different magnifications and it is hard to determine whether or not cross-links between the large fibers are present due to the matrix obscuring the view. Table 3.2 shows the average values observed of trial 2 tube fiber length and diameter. Figure 3.4 shows the trial 2 sample interior in 63x magnification and under regular light.

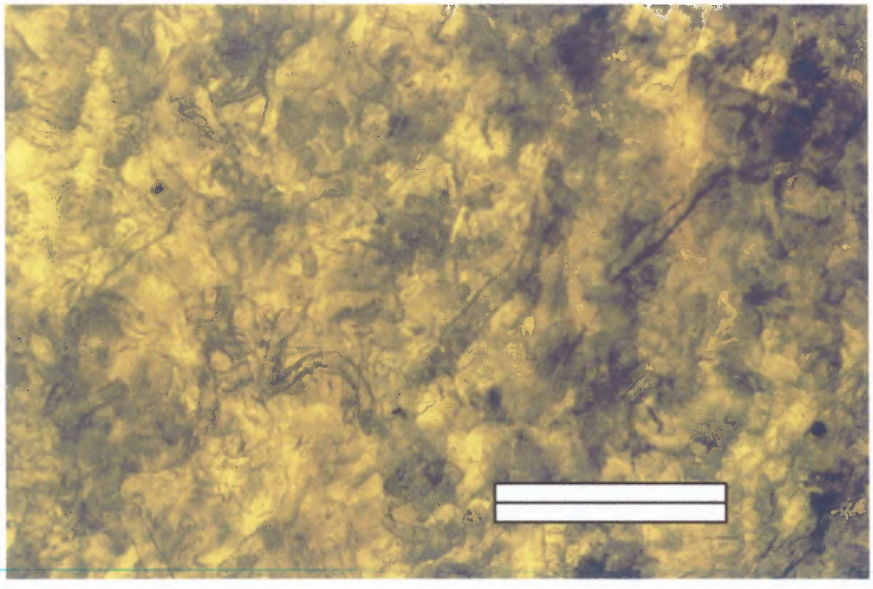

Figure 3.3 Trial 1 collagen tube interior (medium sized tube) shown under regular light at 63x magnification. (Note: Marking is 0.5mm to show scale.)

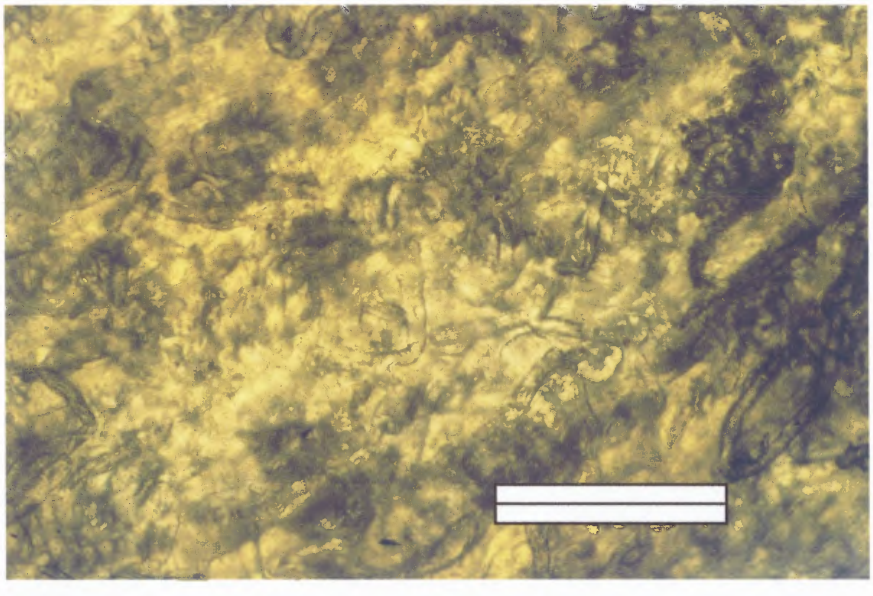

Figure 3.4 Trial 2 collagen tube interior (thin sized tube) shown under regular light at 63x magnification. (Note: Marking is 0.5mm to show scale.)

3.2.4 Trial 3 Tubes

The trial 3 tubes were the thickest and the color of the photo showed a darker shade of yellowish red. Due to the difficulty of light to penetrate the tube and insufficient light reflected onto the surface the fibers were harder to see in the photographs. Once again there was no specific arrangement seen on this interior of the tube photograph of the collagen fibers and as in the other two trials, the fibers run through various planes to reinforce the matrix material. There is no visible smaller fiber cross-links on these photographs but this may be due to the dark background matrix obscuring the image. Finally, there is no difference seen between the fiber structure at different magnifications. Table 3.2 shows the average values of fiber length and diameter for trial 3 tubes. Figure 3.5 show the trial 3 sample in 63x magnification and under regular light.

3.2.5 Exterior Shots of Collagen Tubes

In order to determine whether or not there was any arrangement of fibers caused by the extrusion process, the exterior surface of the collagen tubes were also examined. The exterior shots of the collagen tubes show a more arranged and linear pattern of surface fibers for all three trials. There are also some larger fibers that are at various angles to the general direction line and attach between two fibers arranged in the direction of the line. Fiber lengths and diameters are comparable with those found in the individual trials and will therefore not be presented again. This exterior surface was exposed, in the extrusion process, to the rotating head and would show the fiber alignment more than the interior surface which experienced no forced alignment. Figure 3.6 - 3.8 shows the all three trial sample exterior shots under 63x magnification and regular light.

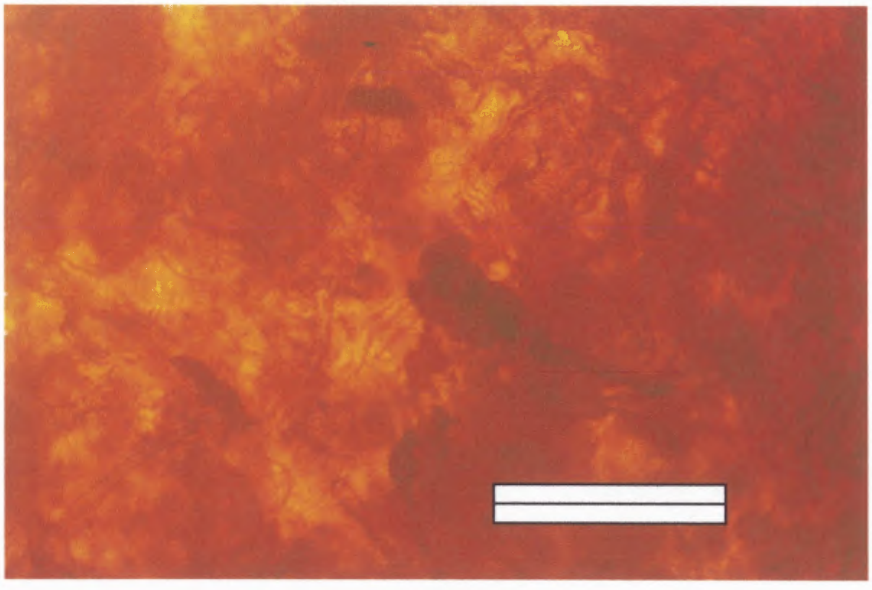

Figure 3.5 Trial 3 collagen tube interior (thick sized tube) shown under regular light at 63x magnification. (Note: Marking is 0.5mm to show scale.)

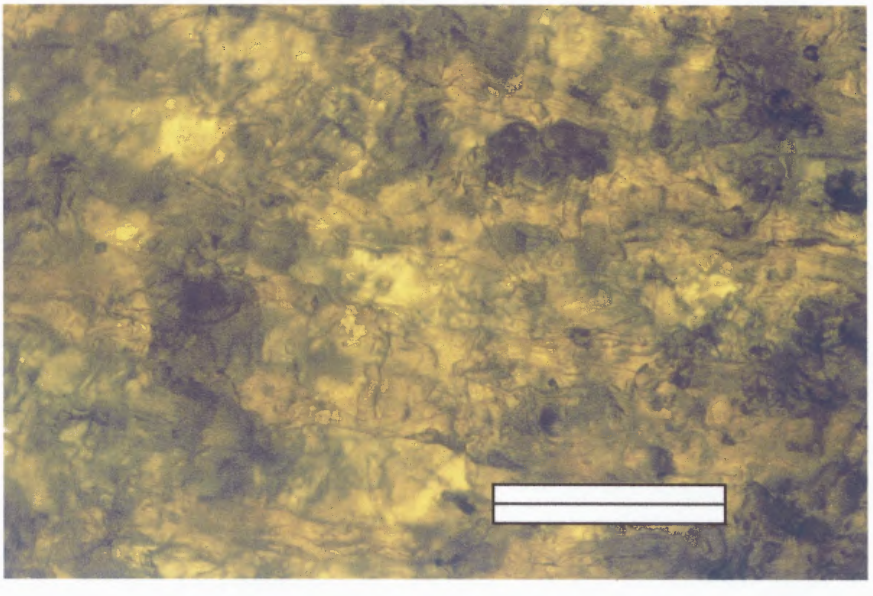

Figure 3.6 Trial 1 collagen tube exterior (medium sized tube) shown under regular light at 63x magnification. (Note: Marking is 0.5mm to show scale.)

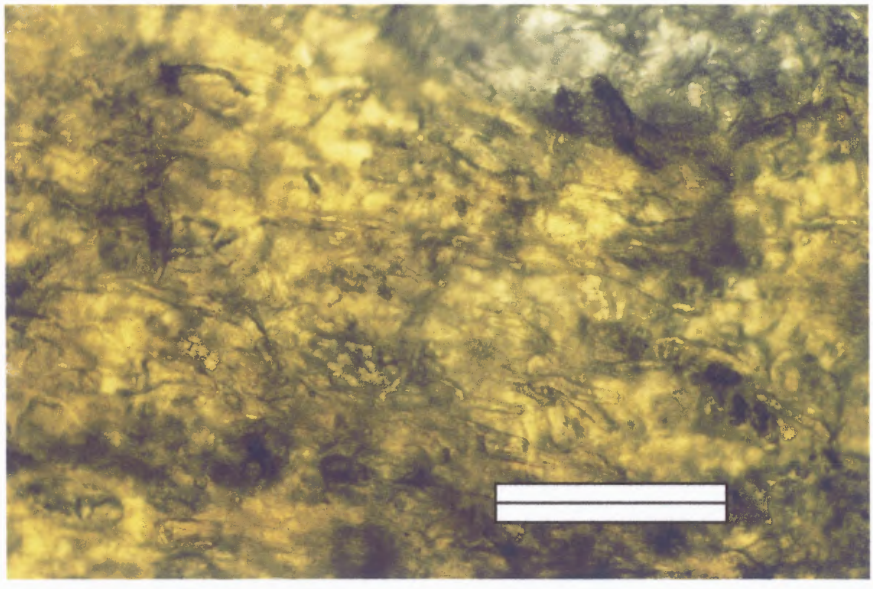

Figure 3.7 Trial 2 collagen tube exterior (thin sized tube) shown under regular light at 63x magnification. (Note: Marking is 0.5mm to show scale)

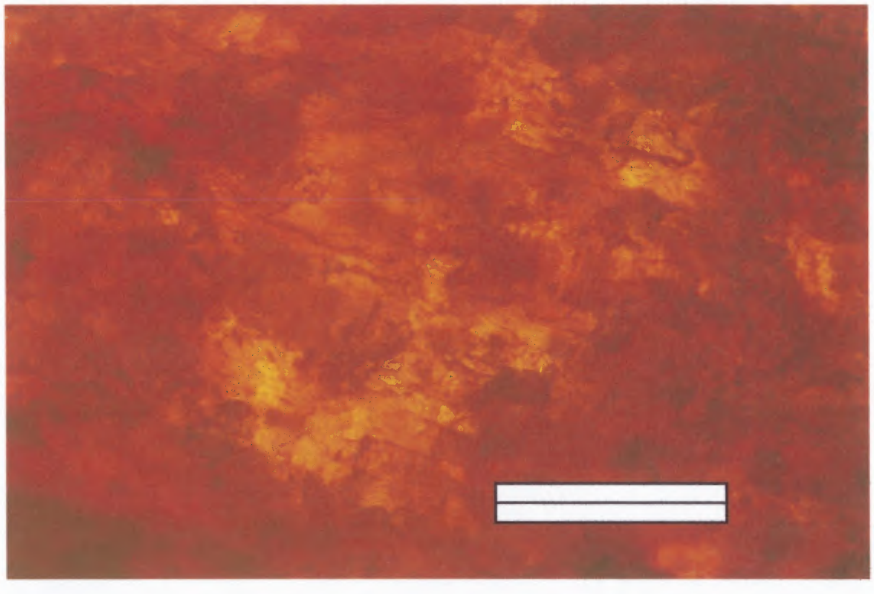

Figure 3.8 Trial 3 collagen tube exterior (Thick sized tube) shown under regular light at 63x magnification. (Note: Marking is 0.5mm to show scale)

3.3 Water Absorption

The water absorption studies were performed on a selected sample of tubes. The mass, length, inner diameter and outer diameter were measured for each tube in a dry state and when wetted for one hour in a water bath. As expected, the mass of a comparable length of thin tube had lower value than that of the medium sized tube which in turn had lower value than the thick tube. Average masses for the three trials, both dry and wet, are shown in Table 3.3. After soaking in the water for one hour and being remeasured, the average volumes for each trial nearly doubled, with 80% change in volume for the medium sized tubes, 105% change for the thin tubes, and 122% volume change for the thickest tubes. Their values are reported in table 3.4.

Table 3.3 Average Mass Dry and Wet by Trial #

	Average Mass Dry (mg)	**Average Mass Wet (mg)**
Trial 1 Tubes	209.09	431.23
Trial 2 Tubes	122.60	244.98
Trial 3 Tubes	418.84	910.80

Table 3.4 Average Volume Dry and Wet by Trial #

	Average Volume Dry (cc)	**Average Volume Wet (cc)**	**Average % Change of Volume**
Trial 1 Tubes	0.191	0.343	80
Trial 2 Tubes	0.121	0.249	105
Trial 3 Tubes	0.368	0.819	123

The density stayed nearly the same between the wet and dry tubes. The length also increased and this can be compared with information regarding the drying of the tubes which was recorded after the initial drying took place. We see that although the numbers vary, there is a general average of about 10% increase in length in the case of

the water absorption and decrease in length (shrinkage) in the case of the drying. Table 3.5a shows the dry and wet density of the tubes and 3.5b the % change in length of both the water absorption trials and the original post-chemical treatment drying.

Table 3.5a Average Density Dry and Wet By Trial #

	Average Density Dry (mg/cc)	**Average Density Wet (mg/cc)**
Trial 1 Tubes	1135.21	1292.67
Trial 2 Tubes	1023.20	1024.46
Trial 3 Tubes	1145.48	1121.95

Table 3.5b Average % Length Change (Comparing Original Drying to Water Absorption Test) By Trial #

	Average % Change in Length (Original Drying) (n=24)	**Average % Change in Length (Water Absorption) (n=4)**
Trial 1 Tubes	13.91	8.38
Trial 2 Tubes	7.07	9.00
Trial 3 Tubes	10.04	13.19

In order to further examine the effects of rotation speed, the data was also averaged by the rotation rate by averaging the values of all the same rotation rates for the three trials. This gave a general view of how the properties at each rotation rate compared with each other independent of what trial they were from. Table 3.6a shows the average volume of the various tubes as arranged by rotation rate. Table 3.6b shows the density and change in length as arranged by rotation rate. The dry volume is pretty consistent between rotation rates between 0.22cc and 0.24 cc. The wet volume, however, shows some differences in the volume with average values ranging from 0.41cc to 0.53 cc. The medium rotation tubes have the highest average volume followed by the low rotation, high rotation and no rotation tubes in order of decreasing volume averages. The percent change in volume shows that they are changing from 76% for the no rotation tubes to

123% for the low and medium rotation tubes and 109% for the high rotation tubes which was consistent with the doubling seen in averages of tubes in the same trial number. The wet and dry densities varied from rotation rate to rotation rate with no noticeable regularity. When examining the average percent change in length the highest change was seen in the medium rotation tube followed by the high rotation tubes, low rotation tubes, and no rotation tubes in decreasing order. The values ranged from 7% to nearly 12 % giving an overall average of about 10% as previously seen.

Table 3.6a Average Volume Dry and Wet By Rotation Rate

	Average Volume Dry (cc)	**Average Volume Wet (cc)**	**Average % Change of Volume**
No Rotation	0.23	0.41	76
Low Rotation	0.22	0.49	123
Medium Rotation	0.24	0.53	123
High Rotation	0.22	0.46	108

Table 3.6b Average Density and Change in Length By Rotation Rate

	Average Density Dry (mg/cc)	**Average Density Wet (mg/cc)**	**Average % Change In Length**
No Rotation	1010.40	1263.17	7.33
Low Rotation	1216.30	1245.87	10.42
Medium Rotation	1050.83	926.35	11.92
High Rotation	1127.67	1150.07	11.08

3.4 Tensile Tests

Tensile tests were performed on a Tinius Olsen tensile testing machine. Selected tubes from each trial were cut to 4 in. lengths for use in the tensile tester. There were two tubes for each rotation rate, eight tubes total, selected for each trial. Twenty-four total tubes were tested. Although the original testing was done using English units, the values

were converted to the metric system to keep consistent with other tests performed. The values obtained were most likely minimum values due to the possibility that the tubes were damaged by the clamps during the testing process. Figure 3.9 shows a sample of what the tensile testing force vs displacement curves looked like.

3.4.1 Trial 1, 2, 3 Tubes

The medium sized and thin tubes were tested using the 100 lb load cell with a gap of 2 in. set between the two clamps. The thickest tubes, trial 3, were tested using the 1000 lb load cell calibrated to 250 lb for recording purposes. The machine stretched the tube until failure at which time the recorder pen was turned off. Table 3.7 shows the average break values for the different trials. All tubes had a relatively clean transverse break with no visible yield or stretching noted during the running of the experiment. The thinnest tubes had the lowest force required to break, with medium tubes in the middle and thickest tubes requiring the most force to break. The thick tubes required almost double the amount that the medium tubes needed and three times the amount of force needed to break the thinnest tubes.

Table 3.7 Average Break Value By Trial #

	Average Break By Trial (N)
Trial 1 Tubes (Medium)	258.84
Trial 2 Tubes (Thin)	153.97
Trial 3 Tubes (Thick)	486.40

Using the force required to break and the area on which it acts, the tensile strength was found for each of the tubes. An average of the two tubes corresponding to the same rotation rate was made for each trial. These were then averaged again to give the

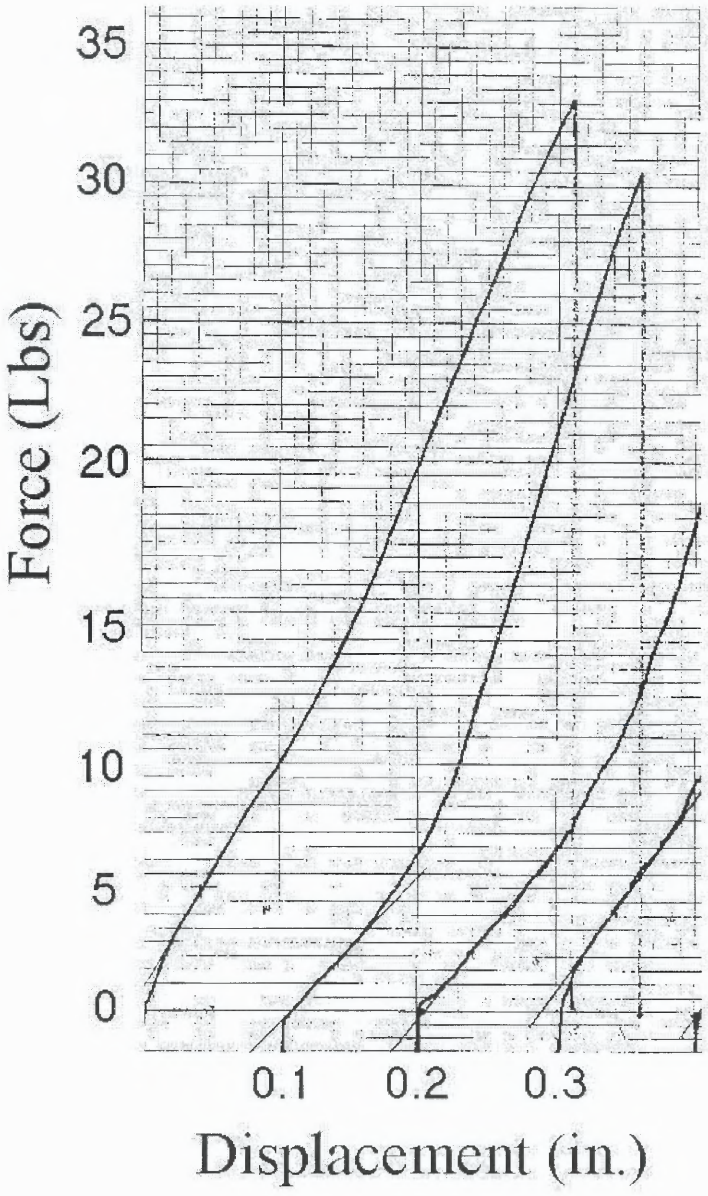

Figure 3.9 Sample tensile curve taken from the trial 2 tubes (thin sized) showing the typical shape of the Force vs. Displacement curve attained during testing. The other sections of curves represent the subsequent tests which were plotted on the same output sheet with a staggered start point and are independent of each other.

average tensile strength of all tubes (regardless of rotation rate) in each trial. The tensile strength values averaged by trial number are reported in table 3.8.

Table 3.8 Average Tensile Strength Values By Trial #

	Tensile Strength Average (MPa)
Trial 1 Tubes (Medium)	18.20
Trial 2 Tubes (Thin)	13.95
Trial 3 Tubes (Thick)	12.98

In order to determine the effects of rotation rate, the tensile strength values of all tubes with same rotation rate were averaged, regardless of trial number. Table 3.9 shows these averaged values by rotation rate. Figure 3.10 shows a graphical representation of the tensile strengths when averaged by rotation rate. By excluding the no rotation rate tubes, the general trend of decreasing tensile strength as the rotation rate increased became apparent. The linear fit value was almost 95% fit of the included data points.

Table 3.9 Average Tensile Strength Values By Rotation Rate

	Tensile Strength Average (MPa)
No Rotation	13.38
Low Rotation	15.89
Medium Rotation	15.85
High Rotation	15.05

Another aspect examined was the modulus of both the initial and end regions. Initial region modulus was calculated from the slope for the first 10% of the force versus displacement curve. The end region modulus was calculated from the slope for the linear portion before break on the same curve. The modulus data was handled in the same manner as the tensile strength data in that averages were found by trial and by rotation

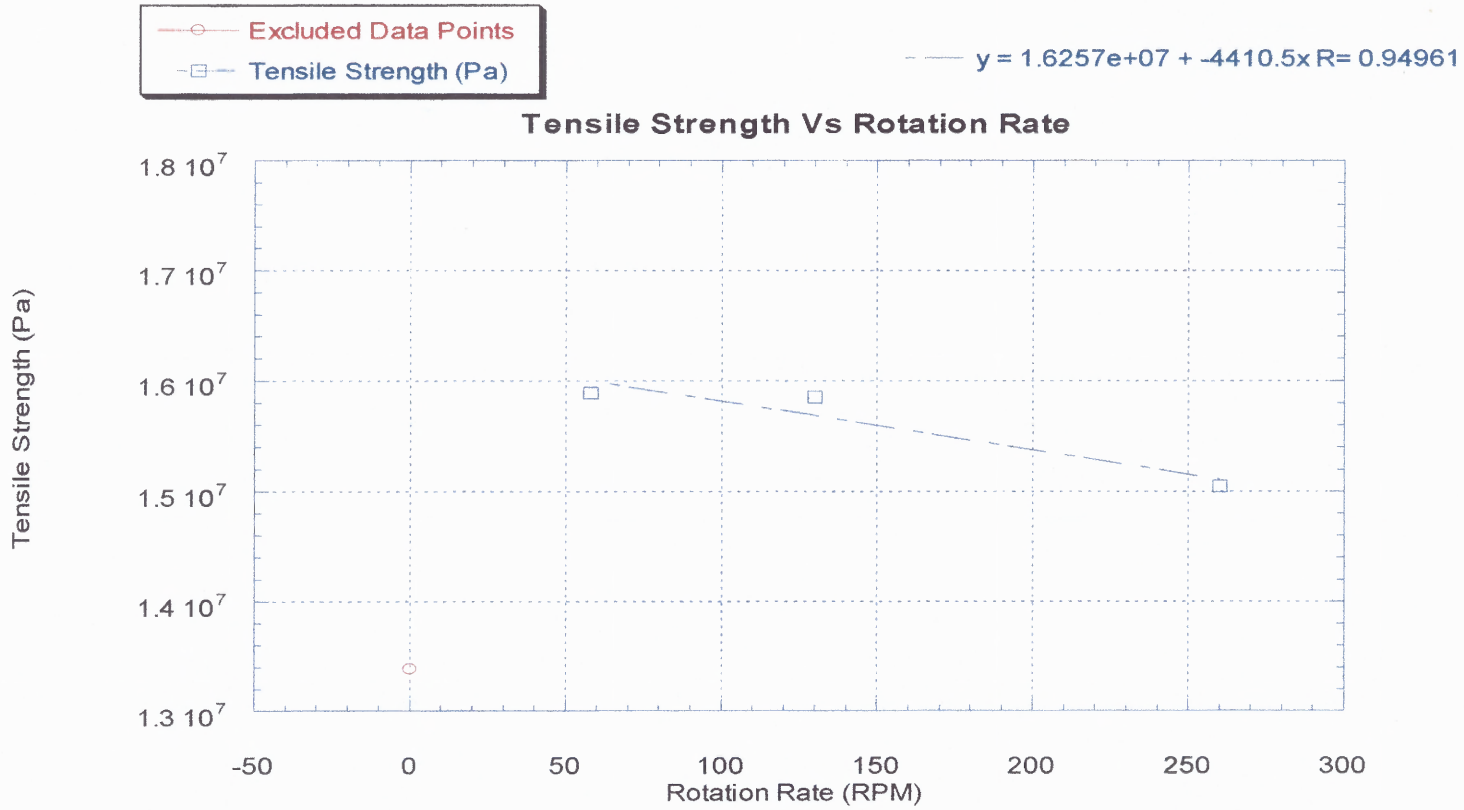

Figure 3.10

Tensile Strength vs Rotation Rate showing the decreasing tensile strength as the rotation rate increases. By excluding the tensile strength of the no rotation rate tubes, we see a 94% fit to the linear relationship of decreasing tensile strength.(Note: No Rotation = 0 RPM ; Low Rotation = 58 RPM ; Medium Rotation = 130 RPM ; High Rotation = 260 RPM)

rate. These values are reported in tables 3.10 and 3.11. Examining the initial modulus, we saw a decreasing modulus from no rotation to low rotation to medium rotation. The high rotation initial modulus broke this trend and was between the value for the no and low rotation moduli. The end modulus, in contrast, showed a regular trend of increasing values as the rotation rate increased. Figure 3.11 shows a graphical representation of these trends along with linear curve fit showing a 97% fit for the end modulus and a 99% fit for the initial modulus excluding the high rotation rate which was plotted as an excluded data point. This initial modulus fit value would be about 24% if the high rotation rate data point was included. Since modulus is a determinate of how elastic the material is, a higher value would represent a more elastic material or region and a lower value is a more brittle material or region. A decreasing average would suggest the initial modulus becoming more brittle as the rotation rates increases. The increasing modulus suggests increasing elasticity of the linear/end region with increasing rotation rate.

Table 3.10 Average Initial and End Modulus By Trial #

	Initial Modulus Average (Pa)	**End Modulus Average (Pa)**
Trial 1 Tubes	3334.167	7802.561
Trial 2 Tubes	1959.392	6278.012
Trial 3 Tubes	3149.662	4148.621

Table 3.11 Average Initial and End Modulus by Rotation Rate

	Initial Modulus Average (Pa)	**End Modulus Average (Pa)**
No Rotation	3245.911	4943.841
Low Rotation	2758.391	5875.484
Medium Rotation	2293.059	6300.827
High Rotation	2960.266	7185.441

By examining the break length and knowing the initial length, the strain can be determined for the tubes. Table 3.12 shows the averaged break lengths and strain by trial and table 3.13 shows them by rotation rate. The medium sized tubes (trial 1 tubes) had the highest average break length followed by the trial 2 tubes and finally the trial 3 tubes. Amongst the rotation rates, there was a general trend of decreasing break length when going from low rotation to high rotation. Since strain was calculated as the change in length divided by the original length, the same trends seen in the length changes are seen in the strain values.

Table 3.12 Average Break Length and Strain By Trial #

	Average Strain (mm/mm)	**Average Break Length (mm)**
Trial 1 Tubes	7.684	7.807
Trial 2 Tubes	7.572	7.693
Trial 3 Tubes	7.050	7.163

Table 3.13 Average Break Length and Strain By Rotation Rate

	Average Strain (mm/mm)	**Average Break Length (mm)**
No Rotation	7.521	7.641
Low Rotation	7.738	7.861
Medium Rotation	7.350	7.468
High Rotation	7.133	7.247

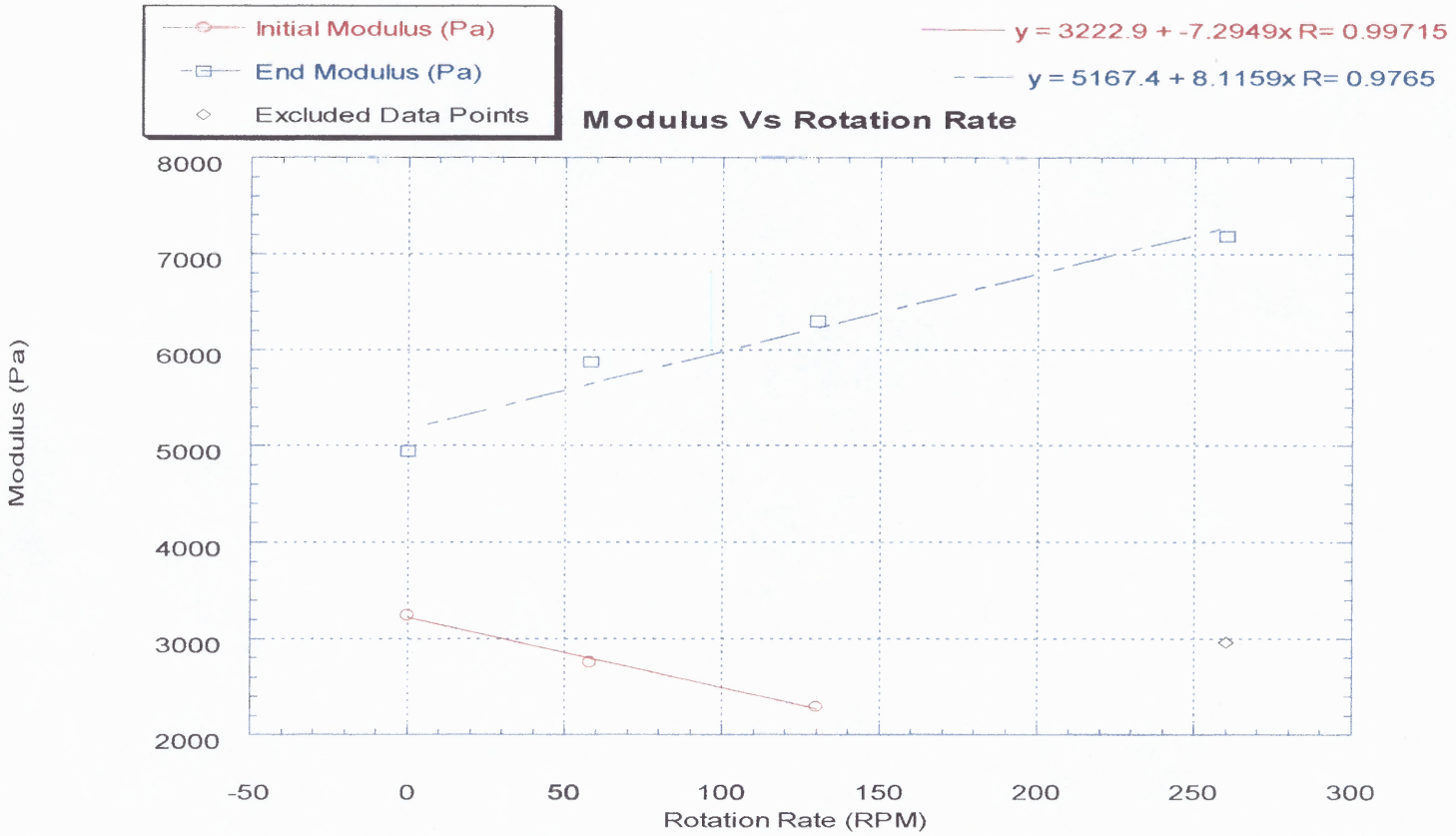

Figure 3.11
Modulus vs Rotation Rate showing the general trend of end modulus average to increase as the rotation rate increases with 97% curve fit. The initial modulus, excluding the final data point, has a 99% fit of the linear trend curve. (Note: No Rotation = 0 RPM ; Low Rotation = 58 RPM ; Medium Rotation = 130 RPM ; High Rotation = 260 RPM)

3.5 DSC Tests

Differential scanning calorimetry testing was done using a Perkin-Elmer DSC7 machine. Plots were made of temperature versus energy for samples from a selection of tubes. There was one tube from each rotation rate tested for each trial for a total of four tubes per trial and twelve tubes total. A second set of plots were made for the tubes which were run under the dehydrated protocol to determine the thermal properties after water had been removed from the collagen matrix.

3.5.1 Non-Dehydrated Tests

The general shape of the non-dehydrated sample curves consisted of several similar shapes as seen in figure 3.12. This is a sample of the DSC curve. All curves showed a water peak in the first region with peaks at around 100° C and various other minor peaks before showing an exothermic region leading to degradation. The water peaks were examined closer to quantify the lower and upper regions for analysis. Table 3.14 shows the values of the average water peak minimum and average maximum when sorted by trial number. Table 3.15 also shows the averages of the minimum and maximum when sorted by rotation rate. No apparent trend was seen between the trial water peak min and max average values except that the medium sized tubes had the highest minimum value and the highest maximum value. The thinner tubes have temperature values less than those of the medium sized tubes but higher than the temperatures at which the water peak started and finished for the thickest tubes. In essence, the order of the water peak from the origin onward was the thickest tubes, the thinnest tubes, and the medium sized tubes furthest from the origin. The breakdown by rotation rate showed more noticeable trends.

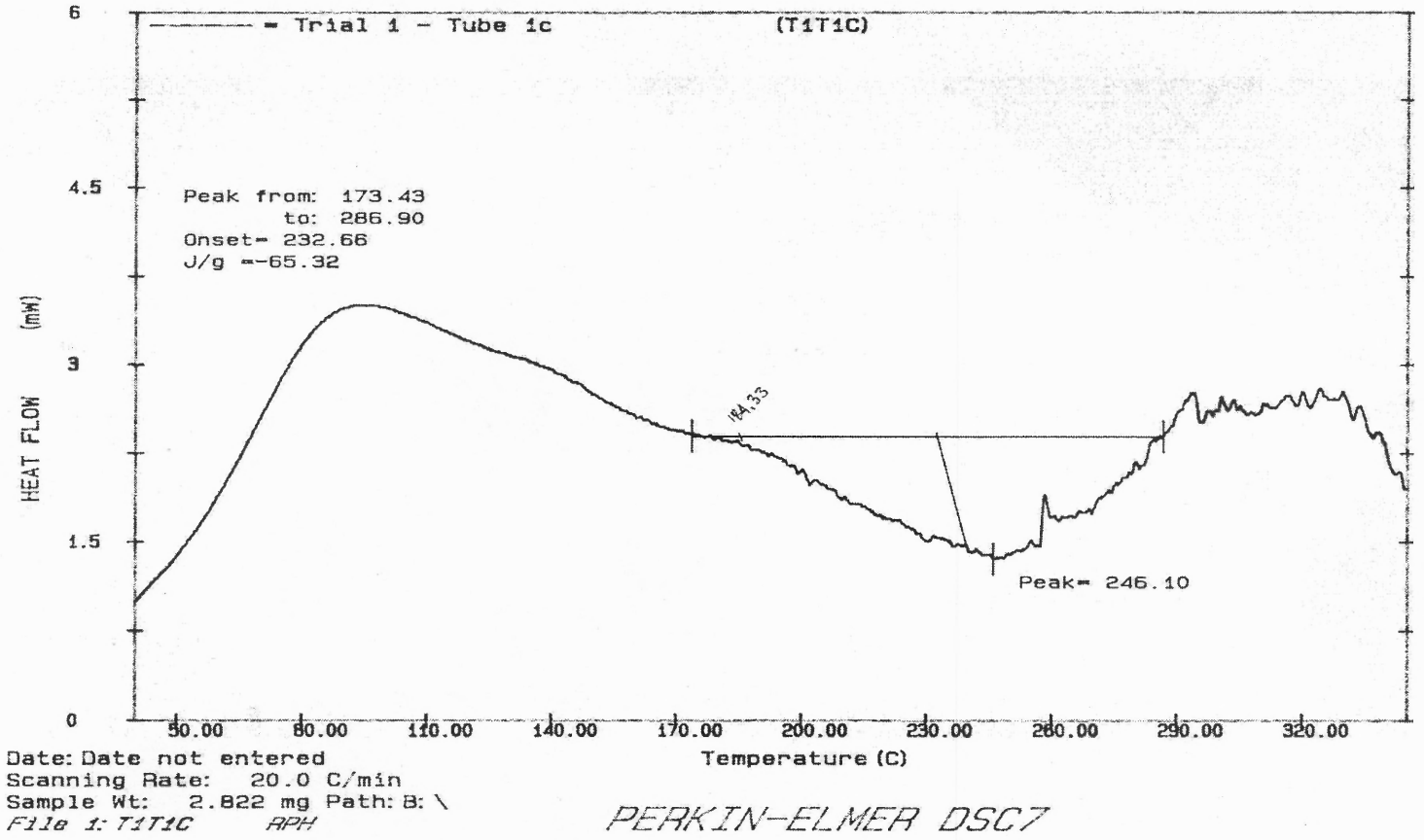

Figure 3.12 Sample DSC curve showing the prominent water peak and exothermic region before final degradation of material.

As rotation rate increased from no rotation to high rotation, the water peak minimum decreased from 51° C to 47° C, 45° C, and 42°C. The maximum value, on the other hand, apparently increased slightly from 174° C to 177° C, 186° C, and 181° C. This phenomenon can be seen in figure 3.13. This suggested that as the rotation rate was increasing, the minimum was lowered and the maximum was raised which gave an overall broader water peak with increasing rotation rate.

Table 3.14 Average Water Peak Minimum and Maximum Values By Trial #

	Water Peak Min Ave (°C)	**Water Peak Max Ave (°C)**
Trial 1 Tubes	55.965	184.503
Trial 2 Tubes	45.943	183.040
Trial 3 Tubes	37.828	171.925

Table 3.15 Average Water Peak Minimum and Maximum Values By Rotation Rate

	Water Peak Min Ave (°C)	**Water Peak Max Ave (°C)**
No Rotation	51.30	174.54
Low Rotation	47.26	177.32
Medium Rotation	45.30	186.38
High Rotation	42.45	181.05

At the end of the water peak, the material produced an exothermic region before the visible high increase in energy absorption associated with degradation began. The peak of the exotherm was in the same temperature range as that of degradation temperature and most likely masked the beginning of degradation. Table 3.16a shows the average value of the exotherm peak when broken down by trial number and table 3.16b by rotation rate. The exotherm peak appeared to increase as the rotation rate increased and, in general, the exotherm value decreased as the tubes got thicker.

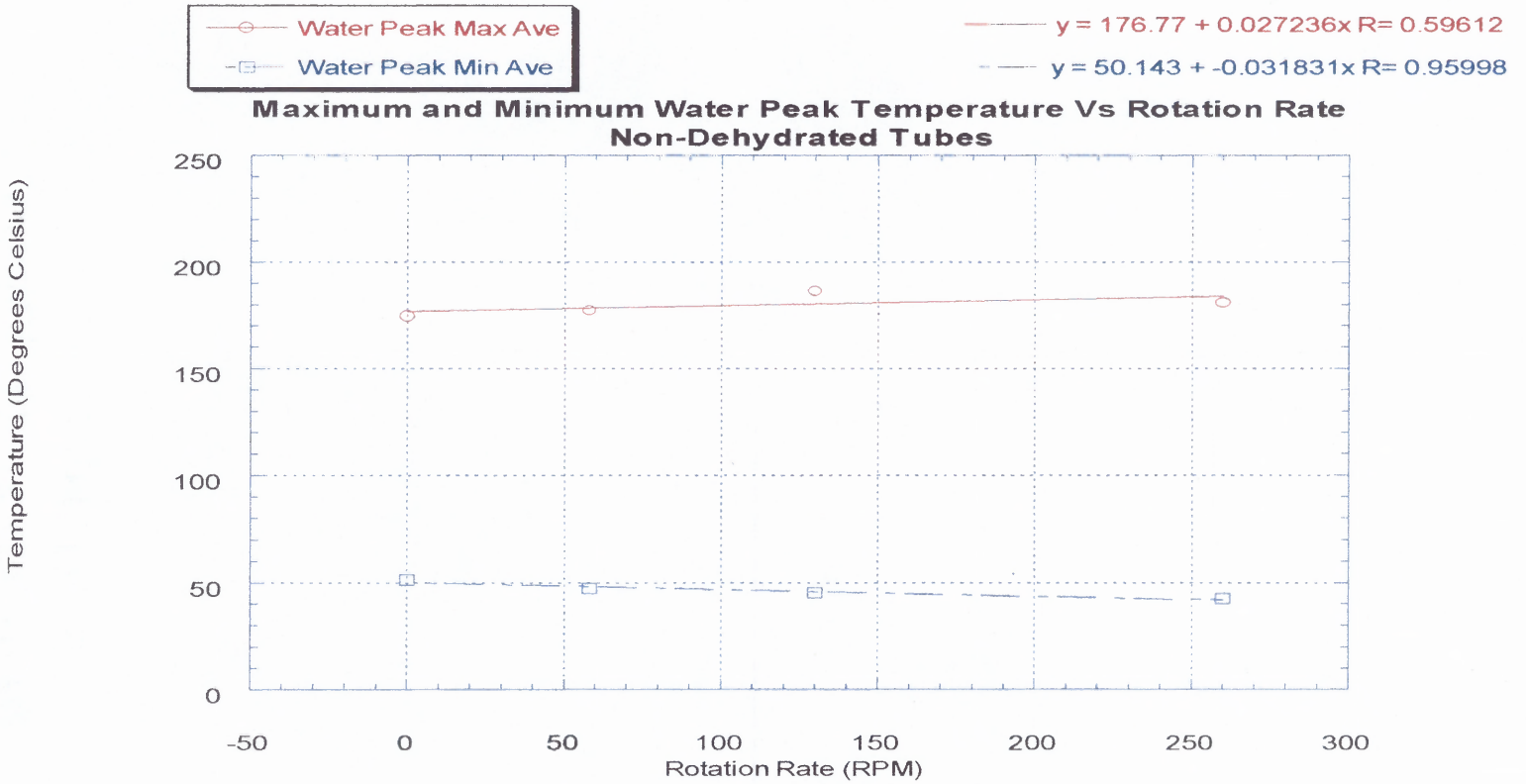

Figure 3.13
Differential Scanning Calorimetry data showing the minimum and maximum water peak temperatures for the non-dehydrated tubes when averaged by rotation rate. We see a general increase in the water peak maximum and a general decrease in the water peak minimum temperatures. The broadening effect of these two trends as rotation rate increases is easily visualized with this graphic representation. (Note: No Rotation = 0 RPM ; Low Rotation = 58 RPM ; Medium Rotation = 130 RPM ; High Rotation = 260 RPM)

Table 3.16a Average Exotherm Peak Value By Trial #

	Exotherm Peak Average (° C)
Trial 1 Tubes	251.85
Trial 2 Tubes	261.05
Trial 3 Tubes	251.34

Table 3.16b Average Exotherm Peak Value By Rotation Rate

	Average Exotherm Peak (° C)
No Rotation	252.57
Low Rotation	253.56
Medium Rotation	256.92
High Rotation	255.93

3.5.2 Dehydrated Tests

The dehydrated tubes were run using the protocol described in the materials and methods section. This was done to examine whether the water peaks could be removed in case they were hiding any other information. The trial 1 and 2 tubes showed reduced water peaks and small exotherms, but the trial 3 tubes showed no water peaks at all and also no exotherm, just degradation at the end region. Table 3.17 shows the average water peak of just the trial 1 and trial 2 tubes so that they can be compared to findings from the non-dehydrated tests. The values for the water peak appear to be narrowing as the tubes get thicker with the thickest tubes having no water peak at all. Table 3.18 shows the water peak minimum and maximum values broken down by rotation rate averages. No trends were apparent in the minimum values, but a general decrease in the water peak maximum temperature as the rotation rate increased was noted. This is the opposite condition as that seen in the non-dehydrated tests and can be seen in figure 3.14. The water peaks were

therefore lessening as the rotation rate increased and the peaks were becoming narrower as the tubes got thicker.

Table 3.17 Average Water Peak Minimum and Maximum Values By Trial #

	Water Peak Min Average (°C)	**Water Peak Max Average (°C)**
Trial 1 Tubes	100.96	154.46
Trial 2 Tubes	63.87	170.46

Table 3.18 Average Water Peak Minimum and Maximum Values By Rotation Rate

	Water Peak Min Ave	**Water Peak Max Ave**
No Rotation	78.72	171.80
Low Rotation	74.61	167.40
Medium Rotation	98.62	156.61
High Rotation	77.72	154.04

The exotherm peaks were noted in the trial 1 and 2 tubes, however the trial 3 tubes showed clearly the temperature at which degradation began. The values for exotherm peak and degradation temperature will be reported in tables 3.19 and 3.20 arranged by trial number or rotation rate. There was no noticeable trend in the exotherm/degradation temperature value averages by trial #. The rotation rate showed a general trend of increased degradation temperature as the rotation rate increased until the highest rotation which had a value between that of no rotation and low rotation. The highest degradation temperature average was 255° C for the medium rotated tubes.

Table 3.19 Average Exotherm Peak/Degradation Temperature By Trial #

	Exotherm Peak Ave (°C)	**Degradation Temp (°C)**
Trial 1 Tubes	250.07	
Trial 2 Tubes	250.32	
Trial 3 Tubes		256.46

Table 3.20 Average Exotherm Peak By Rotation Rate

	Exotherm Peak/Degradation Temperature (°C)
No Rotation	249.46
Low Rotation	252.78
Medium Rotation	255.43
High Rotation	251.46

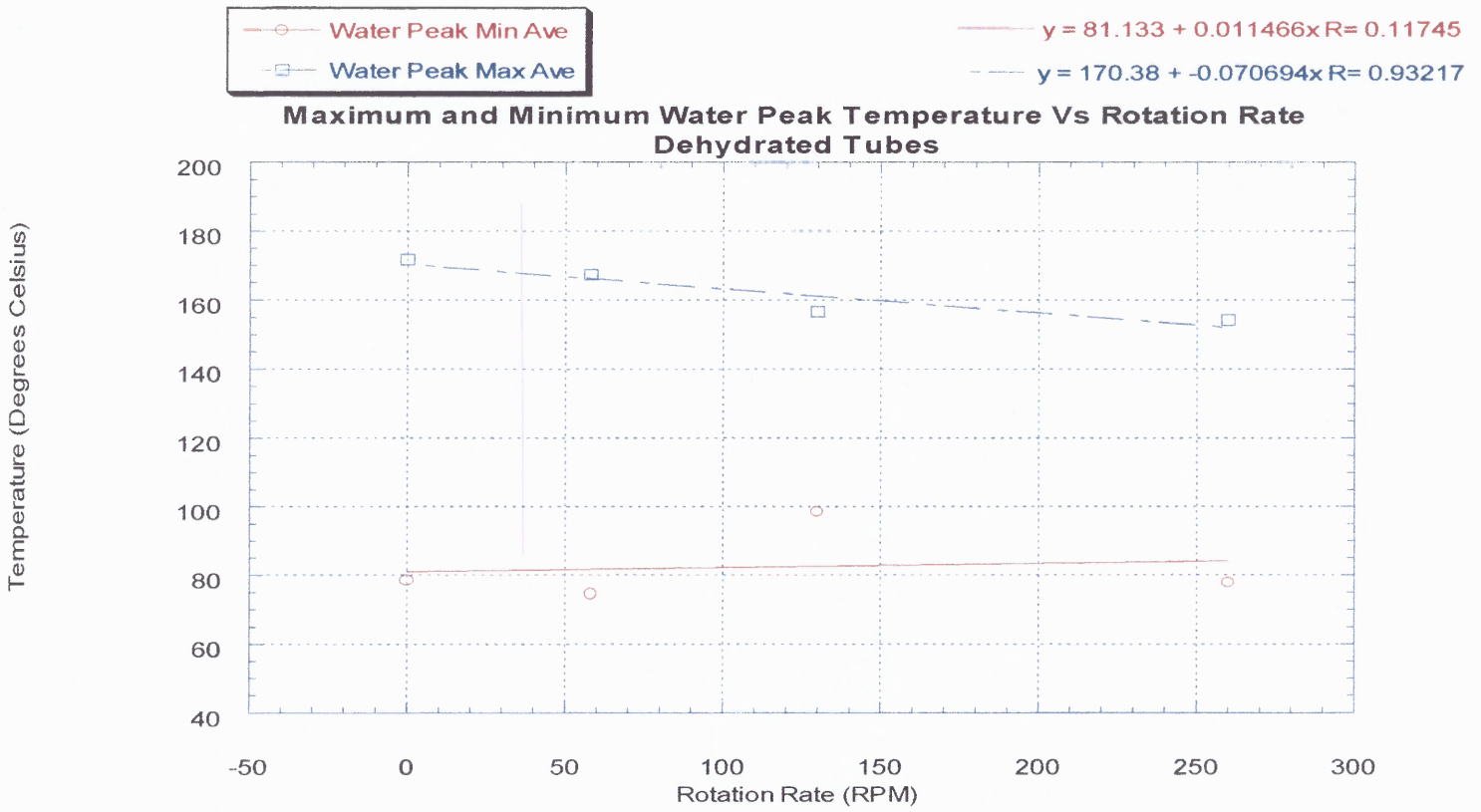

Figure 3.14

Differential Scanning Calorimetry data showing the minimum and maximum water peak temperatures for the non-dehydrated tubes when averaged by rotation rate. We see a general decrease in the water peak maximum and a constant to slight increase in the water peak minimum temperatures. The narrowing effect of these two trends as rotation rate increases is easily visualized with this graphic representation. (Note: No Rotation = 0 RPM ; Low Rotation = 58 RPM ; Medium Rotation = 130 RPM ; High Rotation = 260 RPM)

CHAPTER 4

DISCUSSION

4.1 Extrusion and Chemical Treatment Process

Collagen tubing has multiple applications in the body which require various properties for their success. The first step in evaluating the extruded collagen tubing was to see whether or not it was even possible to make tubes using the extrusion machine. By use of the guide rods and variable settings, the machine was able to create collagen tubing of different thickness and without gaps in the surface that might cause failure. By varying the linear draw speed at which the guide rod was removed from the extrusion head, the thickness of the final tube could be varied. Although not studied in this series of experiments, the adjustment of the collagen extrusion itself should have a similar effect in changing the thickness of the tube. The second variable which was adjustable was the rotation rate of the collagen being deposited onto the guide rods. All the rotation rates tested produced collagen tubing with no visible problems. Since the extreme values of rotation rate were tested, all possible rotation rate values this machine can perform will produce testable and usable tubing.

Although the collagen itself could form into tubes, the removal of such tubes from the guide rods required them to have increased stability and strength. Due to collagen's ability to absorb water into the matrix, it was necessary to chemically treat the collagen tubing with similar processes as would be done for collagen being used in a biological environment. Glutaraldehyde treatment is a common chemical treatment for increasing cross-link density in collagen and thereby making it better able to withstand degradation in liquid environments. The collagen tubes in this study were treated with glutaraldehyde

to make them similar to those that would be used in biological environments as well as make them easier to handle for testing. One immediate observation of the glutaraldehyde treatment, besides color change from white to a yellowish color, was that the re-hydrated tubes still on the guide rods were easier to remove and kept their shape extremely well when compared to earlier tests with non-chemically treated collagen. Sliding the tubes was the only way to remove the intact tubes from the stainless steel guide rod. The process of re-hydration was used since it was observed that the collagen would swell when reintroduced to water and would be easier to slide off of the rods in this swollen state. Unfortunately, the untreated collagen had a tendency to break due to shear forces and friction where the collagen still attached to the guide rod. The shape of the untreated collagen tubes was therefore deformed and it was difficult to get long samples for use in testing. The chemically treated tubes were easier to remove from the guide rods after rehydrating. Unlike the untreated tubes, these tubes held together and the surface did not peel off in layers or break as easily. The structural integrity of the tube was greater than untreated tubes and this allowed them to be slightly twisted to break the bonds with the guide rod and then slide over the surface before final drying occurred. The treated collagen tubes also retained their shape better when dried and did not experience as much curling or collapse due to shrinkage as the untreated tubes did. They did show shrinkage as was expected when most of the water evaporated out of the matrix.

One explanation for the ability of the collagen tubes to retain their shape after allowing them to dry is that the initial drying on the guide rods served as a dehydrothermal cross-linking process as described by various other researchers as a possible treatment (1). In addition to the glutaraldehyde treatment, the drying further

cross-linked the tubes and this made them even better able to withstand shape changes when exposed to water for the rehydration and removal steps. The process was done with all tubes and therefore any comparisons made between different rotation rates or tube thickness should be due to the machine variable changes. The only other consideration which could affect the properties is in the chemical's ability to penetrate adequately into the body of the tube. If the surface absorbs a large amount of glutaraldehyde it can deplete the amount available and prevent further penetration into the sponge giving uneven crosslink distribution (24). This could conceivably lead to the thickest tubes not getting adequate penetration of the glutaraldehyde deep into the matrix. The thinnest tubes would be better able to have full chemical penetration and the properties would show this by having increased cross-links throughout the matrix as opposed to the surface alone. In order to counteract this possibility, the tubes were left in the solution for 10 minutes in an attempt to ensure that the chemical could fully soak into the matrix. In addition, there was adequate chemical in the baths to allow as much as possible to absorb into the tubing. This was achieved by changing the solution for every two rods, allowing a fresh batch to have sufficient concentration of glutaraldehyde. This, however, remained one possible flaw in the chemical treatment which could have seriously affected the properties between the different trials but not as much the tubes with the same thickness but different rotation rate. The only possible effect of rotation rate would be the chemical's inability to pass through due to fiber alignment under high rotation being too close to allow penetration. Since the fibers are randomly dispersed, their ability to completely block the chemical penetration is unlikely.

4.2 Microscopic Studies

In order to examine the collagen tubing and the collagen gel, microscopic studies were done and various photographs were taken both in regular and polarized light. These studies were performed to get a closer look at the matrix and fibers of the collagen gel smeared onto a slide and also within the tubing, both interior and exterior surfaces, to see the effects of extrusion. The fibers in the collagen smear were naturally formed and had the random distribution which was expected due to the slide preparation. Although the fibers did not lie within a single plane, it was possible to make general measurements of the lengths of these natural formed fibers and also determine the thickness. The fibers had an averaged length of 0.57 mm with diameters of 0.046 mm. In general, the length was 10X the diameter of the fiber. This trend was continued with the extruded tubes whose fiber lengths and diameters were nearly identical to the unextruded collagen smear. The corresponding fiber lengths were 0.43mm for trial 1, 0.42mm for trial 2, and 0.42mm for trial 3 tubes. The fiber diameters were 0.051mm for trial 1, 0.0495m for trial 2, and 0.046mm for trial 3 tubes. The fibers thus go relatively unchanged when extruded. Since the fibers are present and there is no noticeable damage, this extrusion process is a viable method for creating fiber-reinforced tubes.

The microscopic studies also showed the arrangement of fibers in the extruded collagen. In general, the interior surface had no regular arrangement of the collagen fibers. The photographs showed the fibers running in various directions and also through various planes although many were running along the plane being examined. This suggests that the collagen fibers are essentially reinforcing not just in the longitudinal plane of the tubes but also in the transverse planes which might help prevent bursting and

extreme changes in dimension to a point. This will have to be further studied to determine if there is a possibility of distributing the fibers throughout the various planes in a regular and ordered manner to aid in raising or lowering properties as the needed for particular applications. As to why there was no linear arrangement of a majority of the fibers, this was most likely due to the fact that this interior surface was simply deposited as extruded onto the guide rod. It was, therefore, not affected by either rotation head or shaping due to passing through the extrusion head known as draw down. The exterior photographs showed a more linear arrangement of the fibers. Since the exterior was directly in contact with the rotating head, it would show the alignment as produced by rotation as well as draw down more so than the interior surface that was already attached to the guide rod.

This explains the linear alignment of the fibers and suggests that the exterior of the tube will have an ability to withstand tensional or burst forces applied to the tube depending on the rotation rate and orientation given due to draw down of the material through the extrusion head. It also suggests that the rotation does cause changes in the alignment of the fibers which can be utilized to change mechanical properties of the tubing. This means that a balance between linear draw down and the rotational depositing of material onto the guide rod can decide the amount of orientation of the fibers in the matrix and give the tube desired mechanical properties. In this way, a higher degree of either orientation will protect the tube either in the lengthwise tensional manner or in burst prevention by aiding in resistance to hoop stress. Hoop stress studies were considered but were left to possible future research and not considered pertinent for this study.

4.3 Water Absorption

The water absorption tests were done to determine whether or not the collagen tubing, when exposed to a liquid environment, would change dimensions causing a problem with the intended application. The volume of the tube did increase due to water uptake by the body of the tube and thus must be accounted for if this were to be used in a biological environment in which space is a consideration. The ability of collagen to swell is not uncommon in liquid environments, particularly in neutral salts or nonelectrolytes and can retain large quantities of moisture (2,25). Its ability to continue to swell even after chemical treatment suggests that the collagen itself is still "active" and able to change. In other words, the chemical treatment did not render the collagen matrix totally impervious to the environment. This suggests that the glutaraldehyde, given sufficient amounts, did penetrate fully into the tubes.

The average volume increase was approximately 100% so the volume of the tubes doubled. The thickest tubes were able to absorb the most water with 123% volume change which might be due to the extra space already present. The thin tubes were able to absorb a higher percentage of water than the medium thickness tubes with a 105% volume change to 80% volume change respectively. When examining the differences between the rotation rates, the tubes which were exposed to no rotation had the lowest volume change with 76%. The low and medium rotation tubes each had 123% volume change and had the highest percent volume change of all the rotation rates. The highest rotation rate tubes were only able to change volume by 105% which suggests that the high rotation rate somehow prevents water from being taken into the matrix possible due to some steric hindrance. The inability of the no rotation tubes to increase in volume may

be due to the cross-linking holding the structure in a tight ladder-like form which doesn't allow as much stretching as the helical cross-linking. This is further emphasized by the low percent change in length recorded for the different rotation rates. The no rotation tubes only had a 7% ability to increase in length suggesting that the absorption of water was not able to stretch the aligned fibers linearly. The higher percentage of length change seen in the medium rotation tubes suggests they absorb water into the matrix and the alignment of the fibers allows for the length of the tube to increase more so than any other rotation rate. With a percent length change of 11.08%, the high rotation tubes are apparently able to change length better than to change volume when compared with other rotation rates. The low rotation tubes with only a 10.4% change in length are less able to change length than other rotated aligned fibers. This suggests that in length change, the low rotation more closely resembles the no rotation tube as far as causes for not being able to expand the longitudinal length of the tube. The medium rotation had the best alignment of fibers for both increasing volume and increasing length. The highest rotation tubes, although not able to expand volume easily, were able to better expand in length possibly due to the ability of the water to separate the cross-links holding fibers which were more closely aligned to the transverse plane.

Besides volume change, the tubes were able to absorb as much water as their own mass, thereby nearly doubling the mass of the entire tube. As expected, the thinnest tubes had the lowest mass and the thickest tubes had the highest mass with the medium thickness tubes having intermediate mass. The density of the dry tubes also showed the trend of increasing with thickness of the tubes when examined by trial number. The density of the wet tubes, however, was increased for the intermediate thickness tubes

when compared to the dry value. The thinnest tube density stayed nearly the same when wet as when dry. The thickest tubes, in contrast, decreased in density when the tubes were wet. This would suggest that the mass of the intermediate tubes were able to increase more than the volume when absorbing water. The mass of water it did absorb was greater than the water's ability to cause a change in the volume which resulted in a greater density when wet than when dry. The thinnest tubes absorbed as much water mass as they were able to increase in volume which helped keep the density of the wet and dry tubes nearly identical. The thickest tubes changed volume more than the amount of water mass they absorbed. This resulted in the lower density of the thickest wet tubes when compared to their dry form. The mass per unit of volume ration changed according to how much water mass they were able to absorb when compared to how much the water caused changes in the volume by stretching the matrix.

4.4 Tensile Tests

Since the mechanical properties of these tubes will help determine the viability in an intended application, tensile tests were performed on the dry samples to examine the tensile strength attainable through the same alterations in rotation rate and linear draw speed. The values were recorded using English units but were converted to the metric system for ease of comparison and unity in this study. The first observation noted was that the breaking force required was larger for tubes with greater thickness, this was expected as the thickest tubes had the most resistance to failure and the thinnest had the least amount of material to withstand failure. The tensile strength averages of all rotation rates in each trial showed the medium sized tubes having the highest value of 18.2 MPa .

The thinnest tubes had an average of 13.95 MPa followed by the thickest tubes with an average of 12.98 MPa. This suggests that the thickest tubes do not support as much force per unit area as the thinnest tubes are able to and both cannot support as much as the medium sized tubes are able to support per unit area. When looking at the rotation rates, the lowest value was seen for the no rotation rate tubes with only 13.38 MPa of force on average. The value of the low and medium rotation tubes were similar with values of 15.89 MPa and 15.85 MPa respectively. The highest rotation tube average was lower with only 15.05 MPa tensile strength. This lower value for the highest rotation rate is most likely due to the low angle at which the fibers lie which makes it easier for the tensile tests to pull apart the cross-links rather than stretching a mixture of reinforcing fibers and cross-links as can be seen in the low and medium rotation rate tubes. The most puzzling finding is the relatively low value for the no rotation tensile strengths and this may be evidence that the fibers alone are not totally capable of giving high tensile strength, but the combination of fibers and cross-links holding together in the longitudinal plane is the better solution to prevent tensile failure. These averages suggest that the highest tensile strength could be attained using a medium thickness tube with either low or medium rotation.

Another important aspect is the modulus of the material to determine how the tube will react when placed in its intended application. Modulus is a measurement of the material's ability to stretch before it fails. Materials with high moduli are able to withstand high stress without considerable changes in length (strain). Higher values are associated with more elastic materials whereas low values are expected of more brittle ones. When examining the modulus of the tubes, two regions were considered. The first

region considered, the initial region, is also known as the toe region and is taken at 10% of the total curve. The second region considered is the linear region of the curves before failure. In general, by looking at the original data curves of force versus displacement, it was easy to determine that the material was brittle in that there was no plastic deformation region in which the material lost its linearity. The material failed before such a region was noted, and this is a common phenomenon in brittle materials such as concrete. The inability of the material to yield before failing suggests that the modulus should be very low for all the tubes. When examining the initial modulus more closely according to trial averages, the lowest value was seen with the thinnest tubes at 1959 Pa. The thickest tubes had a higher modulus average of 3149 Pa and the medium thickness tubes had the highest modulus of 3334 Pa. These values are all relatively low when compared to a material such as stainless steel whose modulus of elasticity averages 200 GPa or even aluminum with 70 GPa (26). The initial modulus, when examined by rotation rate, showed no noticeable trends. The highest was found for tubes with no rotation with a value of 3245 Pa. This was followed by high rotation with 2960 Pa, low rotation with 2758 Pa, and medium rotation with 2293 Pa. The highest initial modulus would therefore be seen in a medium thickness tube with no rotation.

Unlike initial modulus, the end modulus was calculated using the linear region before failure of the tube. When examining the data values by trial number, once again the highest value found was for medium thickness tubes at 7802 Pa. In this instance, the thin tubes follow with a value of 6278 Pa followed by thickest tubes with 4148 Pa. There is a noticeable trend in the average values by rotation rate for end modulus. The values for modulus appear to increase as the rotation rate increases. No rotation had the lowest

value average at 4943 Pa. The values then increased as the low rotation average was 5875 Pa followed by medium rotation with 6300 Pa and the highest rotation with 7185 Pa. This suggests that the tubes with highest rotation rate could resist higher stress per unit of strain than the lower rotation rates. In other words, these tubes were able to stretch more before failure than the other tubes. This is most likely due to the fact that the cross-links are more easily stretched than the fibers themselves which reinforce the matrix. In the case of the no rotation tubes, the matrix was pulling against the fibers aligned in the longitudinal direction. They were not able to stretch considerably and therefore prevented a high modulus value. As the rotation rate increased, however, the cross-links were critical in the resistance to tension as previously stated in the analysis of tensile strength. As a result, the cross-links, being more stretchable than pulling against the main reinforcing fibers, were able to expand to a greater degree and support the tube until failure finally ruptured their attachments.

The final study of tensile properties was that of strain induced in the tubes before failure. Using the displacement portion of the curve, it was possible to determine the change in length of the tube. Since the original length of the tube was already known, strain could be calculated since it is the change in length divided by the original length. The average break length was once again highest for the medium thickness tubes when looking at averages by trial number with a value of 7.81 mm. Accordingly, the strain was also highest for the medium thickness tubes with a value of 7.68 mm/mm. The next highest average was for the thinnest tubes with average break length of 7.69 mm and corresponding strain of 7.57 mm/mm. The thick tubes had the lowest break length average at 7.16 mm and lowest strain at 7.05 mm/mm. When examining the rotation

rates, the low rotation had the highest average break length with a value of 7.86 mm and a corresponding strain of 7.74 mm/mm. The no rotation tubes followed with average break length of 7.64 mm and strain of 7.52 mm/mm. The medium and high rotation rates were the next in order with break lengths of 7.47 mm and 7.25 mm and strains of 7.35 mm/mm and 7.13 mm/mm respectively.

The trends seen support the idea of collagen tubes as a short fiber-reinforced material. As previously discussed, the extrusion and rotation of the collagen creates a balance between the orientation created by the rotating head depositing material onto the guide rod and the linear draw down as the material passes through the extrusion nozzle giving a more linear alignment. This balance is able to change the properties as the rotation rate changes as demonstrated by the results of the study showing, for instance, a low to medium rotation rate giving the highest tensile strengths. This idea of the "middle ground" giving the seemingly best properties is supported by the idea that the extreme values will serve to increase the properties in one direction while leaving the tube susceptible to the other. For example, the high rotation orientation shows lower tensile strength because the balance is shifted towards protection from bursting due to hoop stresses. The no rotation tube fibers, although aligned to protect from tensile stresses, is inadequate due to the total dependence on the fibers alone which can do little to support the matrix material between the fibers. This scenario has little to no support from cross-links which would give added matrix reinforcement in the lengthwise direction and could help hold the tube together longer allowing a higher ultimate tensile strength.

4.5 DSC Studies

The final analysis of the collagen tubes was to determine some thermal properties of the tubes and determine differences between the rotation rates. Two types of tubes were tested, those which were tested without dehydration and those which were exposed to 80°C for 30 minutes prior to testing for purposes of dehydration. As can be seen in the sample DSC curve of the results section, there is a distinct water peak which encompasses the majority of the curve. The non-dehydrated tests show this clearly and this was the reason a second set of DSC tests was performed which attempted to remove most of the water from the collagen tubing in order to remove this water peak.

Examining the water peak was the first objective of the DSC tests. The minimum value was taken as the lowest temperature which showed an increase separate from the baseline value, basically the beginning of the material showing endothermic reactions. The maximum value was taken as closely as possible to when the peak regained the baseline. When examining the averages of all trials the medium thickness tubes show both the highest minimum temperature and maximum temperature starting the water peak at 56°C and ending at 185°C. The thinnest tube water peak average minimum was 46°C with maximum of 183°C. Finally, the thickest tubes showed average water peak minimum of 38°C and maximum of 172°C. Therefore the range of the water peak for the medium thickness tubes was 129°C, the range for the thinnest tubes was 137°C and the range for the thickest tubes was 134°C. It appears as though when comparing the water peaks of the three trials, the ranges are nearly the same but the peaks are simply shifted according to the thickness of the tube. This suggests that the temperature required for

initial release of the water from the matrix is highest for the medium thickness tubes and is lowest for the thickest tubes. Once the water started leaving the matrix, however, the tube thickness had little effect on the range of temperature required before the water was completely removed and no further energy was taken in for shape changes of the matrix molecules.

The dehydrated tests showed no water peak for the thickest tubes and a different range for the water peak minimum and maximum values for the thin and medium sized tubes. The medium sized tubes had a minimum value of 101°C and maximum value 154°C for their water peak which translates to a temperature range of only 53°C. The thinnest tubes had a minimum water peak value of 63.9°C with maximum value of 170°C for a temperature range of 107°C. Both of these ranges were less than those seen in the non-dehydrated test samples, especially if the trial 3 tubes with no water peak are considered. This suggests that the dehydration process did drive out some water from the three sets of samples and that the remaining water did not need as broad a range of temperature to drive to the remaining portion as was needed for the initial tests.

The rotation rate averages for minimum and maximum water peak temperatures showed a trend with relation to increasing rotation rate. In general, as the rotation rate increased, the water peak minimum decreased and the water peak maximum increased. The minimum values changed from 51.3°C to 47.3°C to 45.3°C to 42.5°C when rotation rate went from no rotation to high rotation. In contrast, the maximum peak temperatures went from 174.5°C to 177.3°C to 186.4°C with a minor drop to 181.0°C from no rotation to high rotation. The general effect of such changes is a broadening of the water peak. In other words, the range of temperature in which the no rotation tubes expelled its water

was the thinnest and the high rotation tubes needed the greatest range in temperature to remove all of its water.

The dehydrated tests also showed changing ranges for the water peak when comparing rotation rates. Although the water peak minimum values were relatively stable except for the medium rotation rate average, the maximum values showed a general decrease in the water peak maximum temperature. With values decreasing from 172°C to 167°C to 157°C to 154°C, there is a general narrowing of the water peak. The ranges for the water peaks change from 93.08°C to 92.79°C to 57.99°C to 76.32°C when changing from no rotation to low rotation to medium rotation to high rotation. The only discrepancy is the medium rotation. In essence, by treating these tubes to heats of 80°C for thirty minutes in an attempt to drive off the water, the ability of the samples to later remove the rest of the water was changed by narrowing the temperature range needed to expel the remaining water. The values also required higher minimum start temperatures before water was removed than the initial tests. One interesting observation is that the minimum temperature where the water peak started to rise was near the 80°C mark which was used to drive the water out and suggests that the rise to the temperature was able to remove a particular amount of water but was not enough energy to cause changes which would allow further water to be removed. Once the final test was run, the higher temperatures provided sufficient energy to remove the remaining water suggesting that there are distinct regions with which water resides in the matrix. Perhaps the energy requirements to cause these regions to be removed are higher due to the necessity of forcing more and more of the matrix to change conformation to allow the water to exit

the matrix. This may be caused by the processing itself by increasing steric hindrance and preventing the water out, or may be due to cross-linking which could trap more moisture.

One final consideration for these DSC tests was an exothermic region which appeared at the end of all but the thickest dehydrated tubes. This region could have been caused by shrinkage of the collagen matrix/molecule which is a common phenomenon or even some form of denaturation of the material. Some collagens undergo a period of thermal shrinkage the temperature of which is based on the animal source of the collagen (2). For the non-dehydrated tubes averaged by trial number, the thinnest tubes had the highest average value for the peak of this exotherm with a temperature of 261°C, which was most likely the highest point of the suspected shrinkage and the beginning of degradation. The medium and thick tubes both had values of 251°C for their exotherm peaks. The dehydrated tubes showed exotherms at 250°C for the medium and thin tubes and the thick tubes, although showing no real exotherm, did show the degradation temperature of 256°C.

When looking at rotation rates as the averaging factor, the temperature seemed to increase until attaining the medium rotation and then dropped for the high rotation exotherm peak temperature for the non-dehydrated tubes. The dehydrated tubes showed a similar increase in the exotherm peak value with a drop after the medium rotation. For the non-dehydrated tubes, the values rose from 252.6°C to 253.6°C to 256.9°C then dropped to 255.9°C when increasing rotation rate from no rotation to high rotation. For the dehydrated tubes, the values rose from 249.5°C to 252.8°C to 255.4°C then dropped to 251.5°C when increasing rotation rate from no rotation to high rotation. Such as trend suggests that the amount of energy required to degrade the material increases as the

rotation rate increases except when comparing the medium to the high rotation tube. This is true for both "normal" tubes and those exposed to a dehydration protocol. Although these changes are only minor, they do show a possible effect of rotation rate being able to cause stability in the tube which can be further examined for various applications. This might be the thermal equivalent of what was discussed for tensile property changes based on the orientation of the fibers in the reinforcement of the tubes. Perhaps the middle ground for rotation rate also causes favorable changes in the raising of degradation temperature. Overall, the approximate value of degradation for all the tubes averaged was 253.5°C as a good indicator of the degradation temperature for these cross-linked collagen tubes.

4.6 Future Research

Further research is important in determining the full feasibility of these collagen tubes being used in medical applications. For the actual extrusion, this research could examine the possibility of layered tubing with different rotation rates and different directions affecting the exterior and interior surfaces to help the tube further withstand biological degradation and have increased orientation for better mechanical properties through steric hindrance and cross-linking. Another possibility is to look into whether the matrix could support cells between the fibers and within the matrix which might help it be more biocompatible or even bioactive in that it can help promote the body to use the implant to as a stepping stone for regeneration.

In-vivo studies could show a great deal in determining how well the tubes can withstand degradation and the harsh environment within the body for various applications. Testing tubes of different rotation rates and draw speeds within the body can

also help to see the effect processing has on the survivability of the implant. Of course, in-vitro studies can be performed as well with the tubes in a "wet" form which would better show the properties the tube would have in its intended application in the liquid environment within the body. This could be performed by allowing the tubes to soak within a saline solution and then use the same tests performed in this study on these moistened tubes.

Another possible research topic would be examining the effect of processing and different cross-linking techniques to determine if there is a set of ultimate properties which these collagen tubes can attain. Conceivably, any combination of processing and chemical or physical treatment could produce a desired mechanical, chemical, biological, and thermal property once the full range of attainable properties are determined.

The final step, once all of these tests have been performed is to use the collagen tubes extruded using this machine in an actual medical implantation. If this extrusion machine can produce a usable tube for medical applications, it would be a great asset to the future of medicine. The ability of changing some of the variables on the machine to tailor-make a tube with desired properties enhanced by post-extrusion treatment makes this method of creating tubes a relatively quick and easy way to revolutionize the medical industry particularly in heart bypasses. These collagen tubes can be made rather rapidly needing only a source of collagen and a guideline for the machine settings needed and the post-extrusion process. Should it prove feasible, harvesting of autografts, xenografts, and homografts may no longer be necessary. Future studies may even look into other possible uses for collagen tubes, fibers, and even films to further change the face of medicine and biomedical engineering.

CHAPTER 5

CONCLUSIONS

The collagen tubing extruder made by the ZOKO corporation has been commissioned and protocols for operation have been established for the purposes of this thesis. Using the extruder, collagen tubes can be formed using a viscous collagen base material and stainless steel guide rods. This study has shown that tubes can be formed with changes in rotation rates from 0 rpm to 260 rpm and linear draw speeds from 383 mm/min to 1270 mm/min with a constant extrusion rate of 50 cm^2/min. Tubes with combinations of any of the rotation rates and draw speeds within these ranges should produce usable tubes for testing. Thickest tubes were produced using the lowest linear draw rate and thinnest tubes were produced with the highest linear draw rate.

Post-extrusion, it was found that chemical crosslinking of the collagen was able to increase the cohesiveness and mechanical integrity of the tubes making them easier to remove from the guide rods and less likely for them to lose their shape. A noted side effect of the chemical treatment was a change in color from an opaque white to a yellow or yellow/red color. Microscopic photographs confirm higher machine directed orientation of the fibers on the surface due to the rotating head and the effect of draw down through the extrusion head. The interior of the tube shows less guided orientation which was based on deposition of material from the rotating head directly onto the stainless steel guide rod.

The collagen tubing displayed high affinity for water and therefore moisture uptake which was able to change the mass by at least 100%. The volume changes of the tubes ranged from 80% to 123% with length changes from 8% to 13% depending on the

original thickness of the tube from medium sized tubes to thin tubes to thick tubes. Similar percentages were seen based on rotation rate.

The tensile properties of the tubes reflect the nature of the tubes as having short fiber-reinforcement. The maximum tensile strength is at the low to medium rotation rate and a medium thickness tube. There is an increasing modulus of the initial toe region as the rotation rate increases. Conversely, the end region modulus decreases as the rotation rate increases. These facts support the idea that the orientation of the fibers and crosslinking in the tubing adjust mechanical properties making the extreme processing conditions less favorable when compared to the low or medium rotation rates. The "middle ground" is able to provide a balance of properties in different directions which is superior to primary support in only the longitudinal (lengthwise) direction or in the transverse direction.

Thermal analysis showed differences between the shapes of energy versus temperature curves when comparing the tubes which were "normal" and those which were heated to drive moisture out of the matrix (dehydrate the tube) before testing. Distinct water peaks appear in non-dehydrated tubes and the range of the water peak temperatures increases as the rotation rate increases thereby broadening the water peak. The minimum values ranged from 42° C to 51° C from high rotation to low rotation and the maximum values ranged from 174° C to 181° C from low rotation to high rotation. The dehydrated tubes showed less distinct water peaks and the range of the water peaks decreased as the rotation rate increased which slightly narrowed the water peak. The minimum water peaks ranged from 74° C to 98° C from low to medium rotation with the

other two rotation rates having values in between. The maximum water peak values ranged from 154° C to 171° C from high rotation rates to no rotation.

The thermal analysis studies also showed an exothermic region which was either some form of shrinkage or denaturing/degradation of the collagen molecules. The actual degradation of the material had a beginning range of temperatures from 250° C to 257° C which apparently increased with increasing rotation rate. The specific values were 252° C for no rotation which increased to 253° C for low rotation, 257° C for medium rotation, and dropped to 256° C for high rotation tubes for the non-dehydrated tubes. The specific values were 249° C for no rotation which increased to 253° C for low rotation, 255° C for medium rotation, and dropped to 251° C for high rotation tubes for the dehydrated tubes.

REFERENCES

1. Rattner, Buddy et al. Biomaterials Science, Academic Press, N.Y., 84-92, 287-288, 1996.

2. Mark, H., Gaylord, N., and Bikales, N., Collagen in Encyclopedia of Polymer Science and Technology, Interscience Publishers, N.Y., 1-15, 1966.

3. Kroschwitz, J., Collagen in Encyclopedia of Polymer Science and Engineering, Volume 3, Wiley Interscience Publishers, N.Y., 699-725, 1985.

4. Orten, J. and Neuhaus, O., Specialized tissues and body fluids in Human Biochemistry, C.V. Mosby Company, MO., 400-406, 1982.

5. Mayne, R., Burgeson, R., Structure and Function of Collagen Types, Academic Press, N.Y., 1-36, 1987.

6. Jain, M., P.H.D. Thesis: Micromechanical Properties of Collagen. Biomed. Eng. Dept., Rutgers, The State University, N.J., 1-23, 1989.

7. Rawn, J.D., Protein conformation and function in Biochemistry, Neil Patterson Publishers, N.C., 86-93, 1989.

8. Ramachandran, G.N. and Reddi, A.H., Biochemistry of Collagen, Plenum Press, N.Y., Chapter 1, 1976.

9. Sasaki, M., Takeda, S., Kato, T., Matsuba, K., Antigenicities of stem bromelain. Contribution of three-dimensional structure and individual amino acid residues, *Journal of Biochemistry (Tokyo)*, 87(3), 817-824, 1980.

10. Wang, M.C., Pins, G.D. & Silver, F., Collagen fiber with improved strength for the repair of soft tissue injuries, unpublished,1-11, 2000.

11. Khor, E., Methods for the treatment of collagenous tissues for bioprostheses, *Biomaterials*, 18, 95-105, 1997.

12. Weadock, K., Olson, R.M. & Silver, F., Evaluation of collagen crosslinking techniques, *Biomater Med Devices Artif Organs*, 11(4), 293-318, 1983-1984.

13. Ruijgrok, J.M., de Wijn, J.R. & Boon, M.E., Glutaraldehyde crosslinking of collagen: Effects of time, temperature, concentration and presoaking as measured by shrinkage temperature, *Clin Mater*, 17(1), 23-27, 1994.

14. Cheung, D.T., Perelman, N., Ko, E. & Nimni, M., Mechanism of crosslinking of proteins by glutaraldehyde III Reaction with collagen in tissue, *Connec Tissue Res*, 13, 109-115, 1985.

15. Szycher, M., High Performance Biomaterials, Technomic Publishing, PA., 111-115, 171-184, 428-429, 1991.

16. Kithara, A.K., Suzuki, Y., Oi, P. et al., Facial nerve repair using a collagen conduit in cats, *Scandinavian Journal of Plastic and Recon Sur and Hand Sur*, 33(2), 187-193, 1999.

17. Mallick, P.K., Fiber-Reinforced Composites, Marcel Dekker Inc., N.Y., 1-20, 1988.

18. Ausias, G., Vincent, M., Optimization of the Extrusion Process for Glass-Fiber-Reinforced Tubes, *Jour Thermoplastic Comp Mater*, 8, 435-448, 1995.

19. Soden, P.D., Kitching, R., Tse, P.C. & Tsavalas, Y., Influence of Winding Angle on the Strength and Deformation of Filament-Wound Composite Tubes Subjected to Uniaxial and Biaxial Loads, *Compos Sci and Tech*, 46, 363-378, 1993.

20. Komanowsky, M., Production of comminuted collagen for novel applications. *J. Am. Leather Chemistry.*, 69, 410-411, 1974.

21. Weadock, K.S., M.S. Thesis: Evaluation of crosslinking procedures used in the design of a collagen-based dermal equivalent. Biomed. Eng. Dept., Rutgers, The State University, N.J., 1-15, 1983.

22. Whyne, C., M.S. Thesis: Evaluation of Crosslinking Methods and Characterization of Surface Features of a Collagen-Based Dermal Equivalent. Biomed. Eng. Dept., Rutgers, The State University, N.J., 1-16, 1984.

23. Kuhn, K., Chemical properties of Collagen in Immunochemistry of the Extracellular matrix. Volume 1: Methods. H. Furthmayr, ed. CRC Press Inc., FL., 2-29, 1982.

24. Cheung, D.T., Nimni, M.E., Mechanism of crosslinking proteins by glutaraldehyde. II. Reaction with monomeric and polymeric collagen. *Connective Tissue Res.*, 10, 201-216, 1982.

25. Parry, D.A.D., Creamer, L.K., Fibrous Proteins: Scientific, Industrial and Medical Aspects Vol. 1, Academic Press, N.Y., 136-147 & 257,1979.

26. Beer, F., Johnston, E.R., Mechanics of Materials 2nd Ed., McGraw-Hill Inc., N.Y., 701, 1992.

27. Mathews, C., van Holde, K.E., The three-dimensional structure of proteins in Biochemistry, Benjamin Cummings Publishing Co., MA., 183-184, 1990.

28. Simmons, D.M., and Kearney, J.N., Evaluation of collagen crosslinking techniques for the stabilization of tissue matrices, *Biotechnol Appl Biochem,* 17, 23-29, 1993.

29. Hohne, G., Hemminger, W. & Flammersheim, H.J., Differential Scanning Calorimetry: An Introduction for Practitioners, Springer, N.Y., Chapter 2, 1996.

30. Reed, R., Science for Students of Leather Technology, Pergamon Press, N.Y., Chapter 6, 1969.

31. Smith, W., Mechanical Properties of Metals in Principles of Materials Science and Engineering, McGraw-Hill Inc., N.Y., Chapter 6, 1986.

32. Tiktopulo, E.I., Kajava, A.V., Denaturation of Type I collagen fibrils is an endothermic process accompanied by a noticeable change in the partial heat capacity, *Biochemistry*, 37, 8147-8152, 1998.

33. Silver, F., Christiansen, D., Biomaterials Science & Biocompatability, Springer-Verlag, N.Y., 97-207, 1999.

34. Kato, Y.P., Silver, F.H., Formation of continuous collagen fibres: evaluation of biocompatability and mechanical properties, *Biomaterials*, 11, 169-171, 1990.

35. Usha, R., Ramasami, T., Effect of crosslinking agents (basic chromium sulfate and formaldehyde) on the thermal and thermomechanical stability of rat tail tendon collagen fibre, *Thermochimica Acta*, 256, 59-66, 2000.

36. McClain, P.E., Wiley, E.R., Differential scanning calorimeter studies of the thermal transitions of collagen, *Jour of Biological Chem*, 247(3), 692-697, 1972.

37. Flandin, F., Buffevant, C., Herbage, D., A differential scanning calorimetry analysis of the age-related changes in the thermal stability of rat skin collagen, *Biochimica et Biophysica Acta*, 791, 205-211, 1984.

38. Samouillan, V. et al., Thermal analysis characterization of aortic tissues for cardiac valve bioprostheses, *Jour of Biomed Mater Res*, 46(4), 531-538, 1999.

39. Pereira, C.A., Lee, J.M., Haberer, S.A., Effect of alternative crosslinking methods on the low strain rate viscoelastic properties of bovine pericardial bioprosthetic material, *Jour of Biomed Mater Res*, 24, 345-361, 1990.

40. Weadock, K.S. et al., Physical crosslinking of collagen fibers: comparison of ultraviolet irradaiation and dehydrothermal treatment, *Jour Biomed Mater Res*, 29(11), 1373-1379, 1995.

41. Chvapil, M., Owen, J.A., Clark, D.S., Effect of collagen crosslinking on the rate of resorption of implanted collagen tubing in rabbits, *Jour Biomed Mater Res*, 11(2), 297-314, 1977.

42. Speer, D.P., Chvapil, M., Eskelson, C.D., Ulreich, J., Biological effects of residual glutaraldehyde in glutaraldehyde-tanned collagen biomaterials, *Jour Biomed Mater Res*, 14(6), 753-764, 1980.

43. Dunn, M.G., Avasarala, P.N., Zawadsky, J.P., Optimization of extruded collagen fibers for ACL reconstruction, *Jour Biomed Mater Res*, 27(12, 1545-1552, 1993.

44. Osborne, C.S., Barbenel, J.C., Smith, D., Savakis, M., Grant, M.H., Investigation into the tensile properties of collagen/chondroitin-6-sulphate gels: the effect of crosslinking agents and diamines, *Med Biol Eng Comput*, 36(1), 129-134, 1998.

45. Koide, T., Daito, M., Effects of various collagen crosslinking techniques on mechanical properties of collagen film, *Dent Mater*, 16(1), 1-9, 1997.

46. Sung, H.W., Chang, Y., Chiu, C.T., Chen, C.N., Liang, H.C., Crosslinking characteristics and mechanical properties of a bovine pericardium fixed with a naturally occurring crosslinking agent, *Jour Biomed Mater Res*, 47(2), 116-126, 1999.

47. Chignier, E., Eloy, R., Hue, A., Gimeno, R., Gleizal, C., Long-term behavior of bovine collagen membrane used as a vascular substitute. Experimental study in rats, *Jour Biomed Mater Res*, 19(2), 115-131, 1985

48. Dalsing, M.C. et al., An experimental collagen-impregnated Dacron graft: potential for endothelial seeding, *Ann Vasc Surg*, 3(2), 127-133, 1989.

49. Werkmeister, J.A. et al., Structural stability of long-term implants of a collagen-based vascular prosthesis, *J Long Term Eff Med Implants*, 1(1), 107-119, 1991.

50. Gratzer, P.F., Pereira, C.A., Lee, J.M., Solvent environment modulates effects of glutaraldehyde crosslinking on tissue-derived biomaterials, *Jour Biomed Mater Res*, 31(4), 533-543, 1996.